

Non-linear Dynamics

Prof. Dr. Ulrich Schwarz

Heidelberg University, Institute for Theoretical Physics

Email: schwarz@thphys.uni-heidelberg.de

Homepage: <http://www.thphys.uni-heidelberg.de/~biophys/>

Winter term 2016/17

Last update: January 25, 2017



Contents

1	The central equation	5
2	Flow on a line	9
3	Bifurcations in 1d	15
3.1	Saddle-node bifurcation	15
3.2	Transcritical bifurcation	19
3.3	Pitchfork bifurcation	21
3.3.1	Supercritical pitchfork bifurcation	21
3.3.2	Subcritical pitchfork bifurcation	22
3.4	Influence of high order terms	22
3.5	Summary of 1d bifurcations	24
4	Flow on a circle	27
5	Flow in linear 2d systems	33
5.1	General remarks	33
5.2	Phase plane flow for linear systems	35
6	Flow in non-linear 2d systems	39

4

CONTENTS

7 Oscillations in 2d **47**

8 Bifurcations in 2d **59**

9 Excitable systems **67**

10 Reaction-diffusion systems **77**

Chapter 1

The central equation

We consider dynamical systems of dimension d which are described by ODEs. This implies that we use continuous time. (One alternative would be different equations with discrete time.) Calling \vec{x} the state vector of the system we consider the equation

$$\frac{d\vec{x}}{dt} = \vec{f}(\vec{x})$$

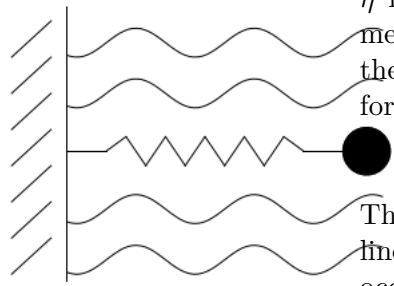
with a vector-valued function \vec{f} which can be non-linear. In case of a linear function \vec{f} the equation simplifies to

$$\dot{\vec{x}} = A \cdot \vec{x}$$

with a matrix A and the system shows exponential behavior.

Examples

1. **Overdamped particle** $\eta \cdot \dot{x} + k \cdot x = 0$



The diagram shows a vertical wall on the left with diagonal hatching. A particle, represented by a black circle, is attached to a spring that is connected to the wall. The spring is shown with a zigzag line. The medium is represented by wavy lines on either side of the particle. The text explains that the system is one-dimensional and linear, and that no oscillations occur due to the overdamping.

η is the viscosity of the surrounding medium. Solving for \dot{x} shows that the equation is already in the general form:

$$\dot{x} = -\frac{k}{\eta} \cdot x.$$

The system is one-dimensional and linear. Because of this, no oscillations occur.

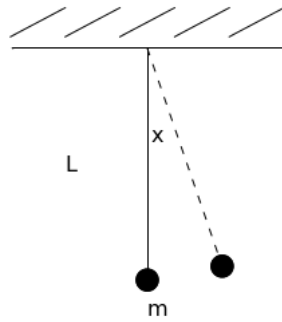
2. **Harmonic oscillator** $\ddot{\vec{x}} + \omega_0^2 \vec{x} = 0$

This looks superficially like an one-dimensional system. But the following trick eliminates the second derivative and shows the linear but two-dimensional character of the harmonic oscillator:

Choose $x_1 = x$ and $x_2 = v = \dot{x}$ with the velocity v . Then, the equation written in the general form is

$$\dot{\vec{x}} = \begin{pmatrix} \dot{x}_1 \\ \dot{x}_2 \end{pmatrix} = \begin{pmatrix} 0 & 1 \\ -\omega_0^2 & 0 \end{pmatrix} \cdot \vec{x}.$$

3. **Pendulum** $\ddot{x} + \frac{g}{l} \sin(x) = 0$

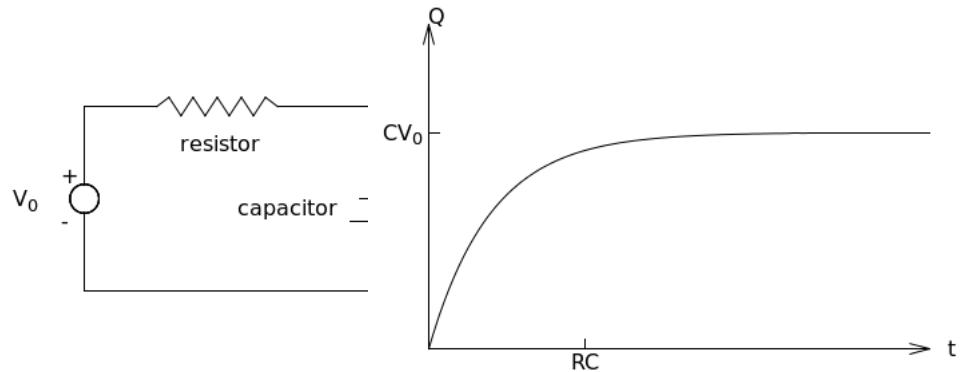


Using the same trick as for the harmonic oscillator, we get $\dot{x}_1 = x_2$ and $\dot{x}_2 = -\frac{g}{l} \sin(x_1)$, hence a non-linear, two-dimensional system. Only for small angles x ($\Rightarrow \sin(x) \approx x$) we end up with a harmonic oscillator.

4. **Driven harmonic oscillator** $m\ddot{x} + k \cdot x = F \cdot \cos(\omega t)$

The equation of the driven harmonic oscillator explicitly depends on time t . But rewriting the equation using $x_1 = x$, $x_2 = \dot{x}$ and introducing a third variable $x_3 = t$ leads to the relations $\dot{x}_1 = x_2$, $\dot{x}_2 = \frac{1}{m}(-kx_1 + F \cdot \cos(\omega x_3))$, $\dot{x}_3 = 1$. The system is non-linear with $d = 3$.

5. **Electric circuit** $R \cdot I + \frac{Q}{C} = V_0$



Using Kirchhoff's law and the relation $I = \dot{Q}$ we get the ODE of an overdamped particle:

$$\dot{Q} = \frac{V_0}{R} - \frac{1}{RC} \cdot Q.$$

Remember this is a linear, one-dimensional system. If we put in a solenoid the dependence of \dot{Q} will lead to $d = 2$ and oscillations can occur.

Chapter 2

Flow on a line

In this chapter, we are looking at one-dimensional systems. Therefore, the central equation becomes $\dot{x} = f(x)$ with an arbitrary function f .

The first example we want to discuss is non-linear: $\dot{x} = \sin(x)$. The separation of variables leads to

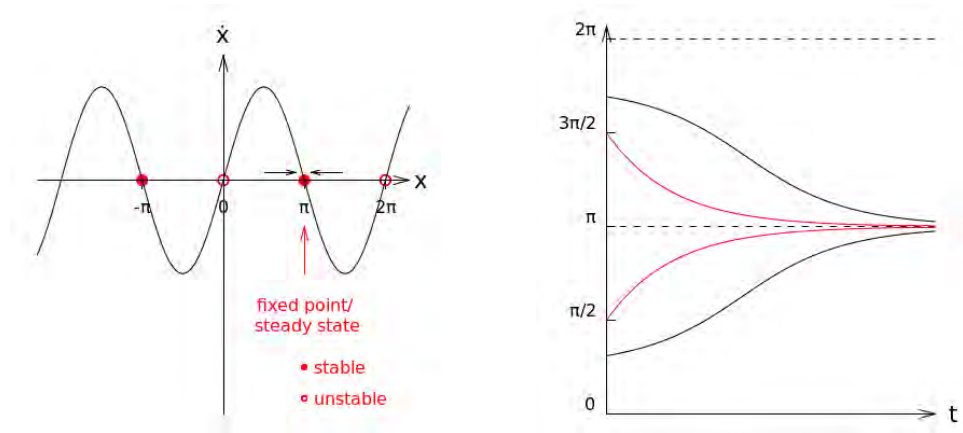
$$\frac{dx}{\sin(x)} = \csc(x)dx = dt$$

which can be integrated with the result

$$t = \ln \left(\frac{\csc(x_0) + \cot(x_0)}{\csc(x) + \cot(x)} \right).$$

Even in this simple non-linear example, the behavior of the system is not easy to understand from this solution. But *graphical analysis* shows the most important properties.

Plotting a phase portrait (left figure), stable and unstable fixed points can be determined. In 1d, the systems dynamics corresponds to flow on the line. The corresponding trajectories are shown in the right figure.

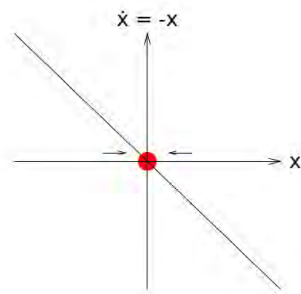


For a stable fixed point a little change in x drives the system back, whereas for an unstable fixed point it causes a flow away from the fixed point.

Choosing different starting points x^* the time-dependence of the acceleration computes as follows: for starting points $|x^* - \pi| \leq \frac{\pi}{2}$ the acceleration directly decreases. But if $x^* = \pi \pm \Delta x$ with $\frac{\pi}{2} < \Delta x \leq \pi$ the acceleration first increases and decreases after the deflection point.

The graphical analysis can be performed for the earlier examples as well:

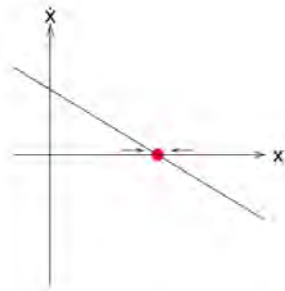
• **Overdamped particle**



$$\dot{x} = -x$$

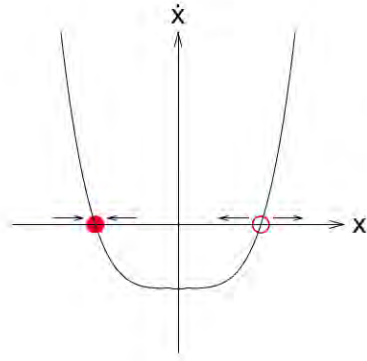
$$x^* = 0, \text{ stable fixed point}$$

• **Electrical circuit**



$$x^* \neq 0$$

The applied method works for any graph.



In an one-dimensional system, there are three possibilities in total the system can behave:

1. staying at a fixed point
2. flowing to a stable fixed point
3. flowing to infinity

There is also a mathematical method to analyze fixed points. It is called *linear stability analysis*. Firstly, one determines the fixed points by solving $\dot{x} = f(x) = 0$ for x . Take x^* to be a fixed point. Then, the deviation η from this fixed point is given by $\eta = x - x^*$.

The derivative $\dot{\eta}$ can be written in dependence of the sum $x^* + \eta$.

$$\dot{\eta} = \dot{x} = f(x) = f(x^* + \eta)$$

The first order Taylor expansion $\dot{\eta} = \underset{=0}{f(x^*)} + f'(x^*) \cdot \eta + \mathcal{O}(\eta^2)$ leads to a first order ODE

$$\dot{\eta} = f'(x^*) \cdot \eta$$

which can be integrated to a time-dependent deviation

$$\eta(t) = \eta_0 \cdot \exp(f'(x^*) \cdot t)$$

with the starting deviation η_0 at $t = 0$. Introducing the *relaxation time* $t_0 = |\frac{1}{f'(x^*)}|$ this yields

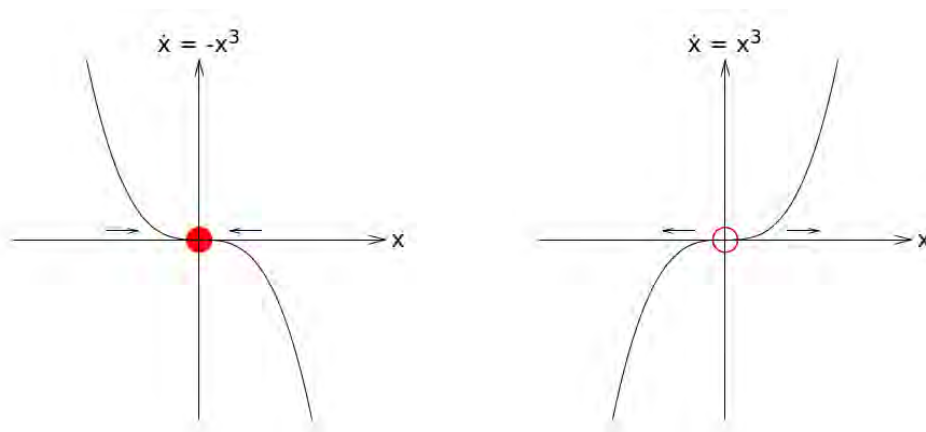
$$\eta(t) = \eta_0 \cdot \exp(\text{sign}(f'(x^*)) \cdot t/t_0).$$

Thus, $f'(x^*)$ hints towards the characteristics of a fixed point x^* .

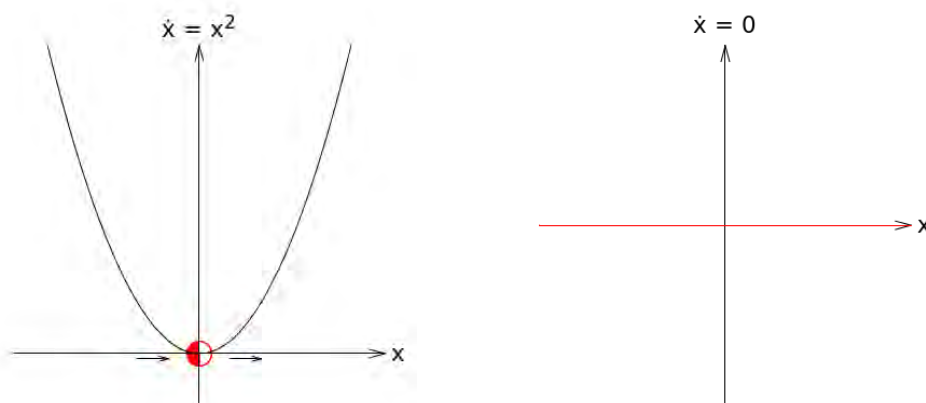
Conclusion

- If $f'(x^*) < 0$: stable fixed point, exponential decay
 $f'(x^*) > 0$: unstable fixed point, blow-up
 $f'(x^*) = 0$: further investigations are needed

Examples



In both cases $\dot{x} = \pm x^3$ the character of the fixed point is not clear from f' .



For $\dot{x} = x^2$ the system has a *half-stable* point at $x = 0$. If \dot{x} is constant, the result is a line of fixed points.

Uniqueness theorem

If $f(x)$ and $f'(x)$ are continuous on an open interval around x_0 , then a solution exists and is unique.

This leads to the impossibility of oscillations in an one-dimensional system. Instead, everything is overdamped. Consider a potential V . In 1d, we can write

$$\dot{x} = f(x) = -\frac{dV(x)}{dx}.$$

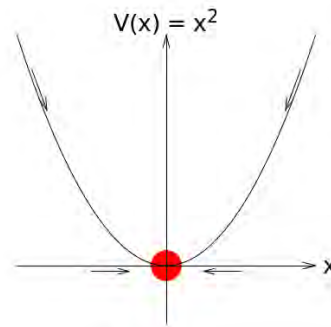
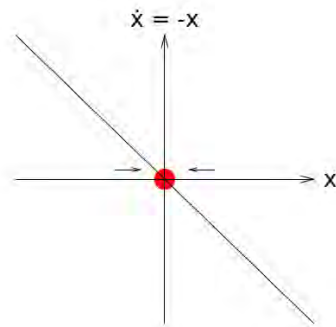
Hence, the time derivative of V yields

$$\frac{dV}{dt} = \frac{dV}{dx} \frac{dx}{dt} = -\left(\frac{dV}{dx}\right)^2 \leq 0.$$

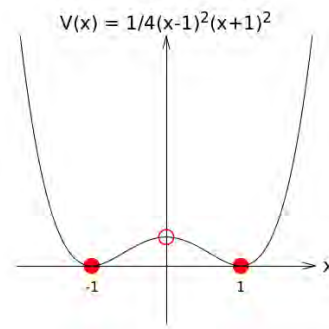
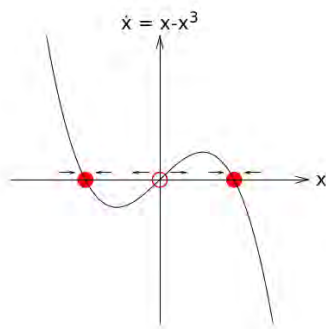
So, the energy of the system can never increase. It always decreases during flow.

Examples

1. Overdamped particle



2. Mexican hat



The Mexican hat is an example of a *bistable* system.

The figures show the following relation for $d = 1$:

minimum in V : stable fixed point
 maximum in V : unstable fixed point

Chapter 3

Bifurcations in 1d

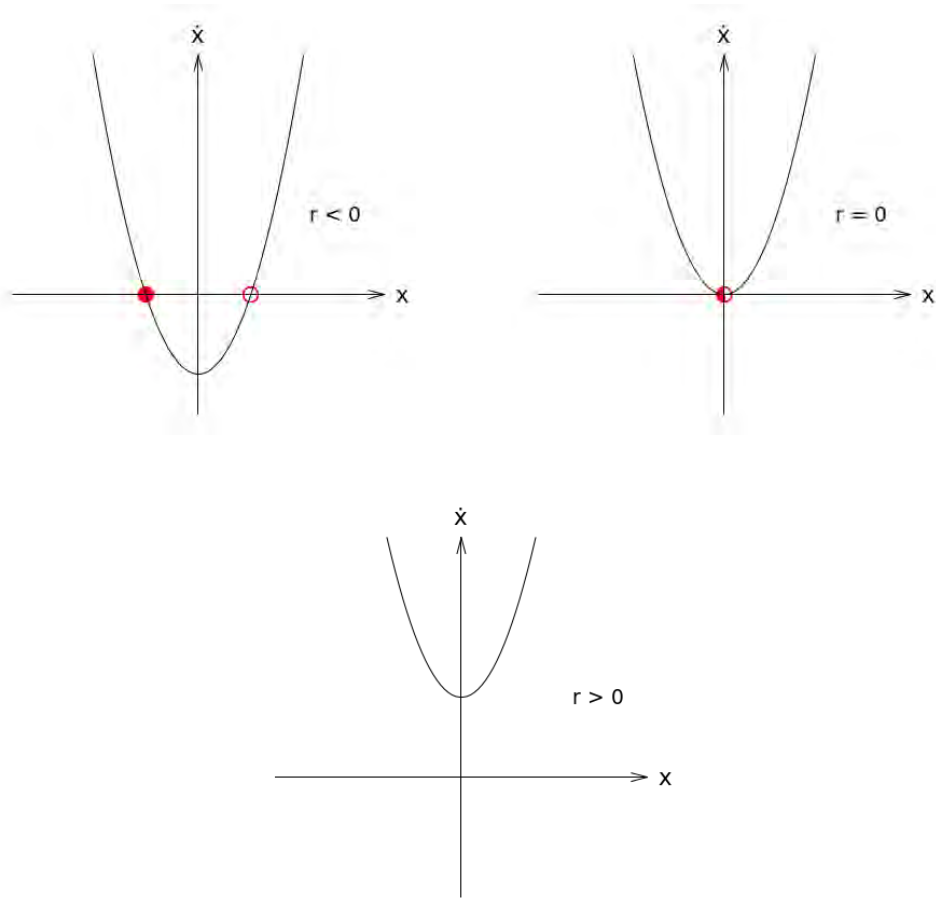
As we have seen in chapter 2, flow can easily be understood in $d = 1$. However, up to now we did not consider any parameter which in principal could change the flow structure. A sudden change in the character of the solution is called *bifurcation*. Physical examples for this are phase transitions, mechanical instabilities, laser thresholds, population thresholds etc.

There are exactly three types of bifurcations in $d = 1$. Mathematically it can be shown that each type can be described by one general form using the bifurcation parameter r . The general properties are summarized in the following table.

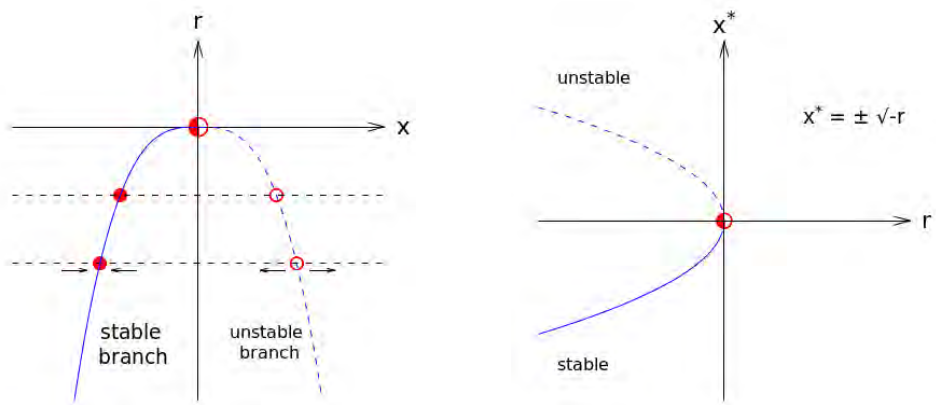
Saddle-node bifurcation	$\dot{x} = r + x^2$	fixed points can appear or disappear depending on r
Transcritical bifurcation	$\dot{x} = rx - x^2$	fixed points always exist for all r but they can exchange stability
Pitchfork bifurcation	$\dot{x} = rx \pm x^3$	fixed points appear or disappear as a symmetrical pair

3.1 Saddle-node bifurcation

Consider $\dot{x} = r + x^2$ with the bifurcation parameter r . The roots are given by $x^* = \pm\sqrt{-r}$. For various r the system behaves differently.

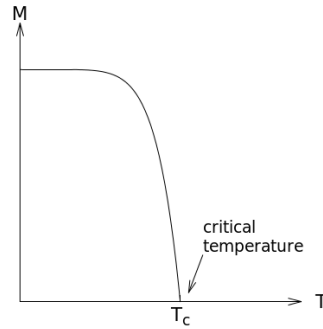


This allows to analyze the influence of r on the flow behavior in a *bifurcation diagram*.

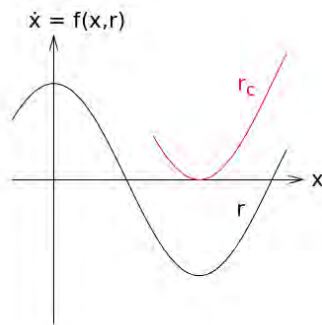


Since the branches appear suddenly for $x^* \leq 0$ the saddle-node bifurcation is also called *out of the blue sky bifurcation*.

This corresponds to a phase transition of second order like the magnetization of an Ising magnet.



But why does $\dot{x} = r + x^2$ describe all saddle-node bifurcations? We assume \dot{x} to be a function of x and the parameter r .



Expanding $\dot{x} = f(x, r)$ around $x = x^*$ and $r = r^c$ leads to

$$\dot{x} \approx f(x^*, r^c) + \frac{\partial f}{\partial x} \Big|_{(x^*, r^c)} \cdot (x - x^*) + \frac{\partial f}{\partial r} \Big|_{(x^*, r^c)} \cdot (r - r^c) + \frac{1}{2} \frac{\partial^2 f}{\partial x^2} \Big|_{(x^*, r^c)} \cdot (x - x^*)^2.$$

Considering $f(x^*, r^c) = 0$ and $\frac{\partial f}{\partial x} \Big|_{(x^*, r^c)} = 0$ the general form computes as

$$\dot{x} = a(r - r^c) + b(x - x^*)^2.$$

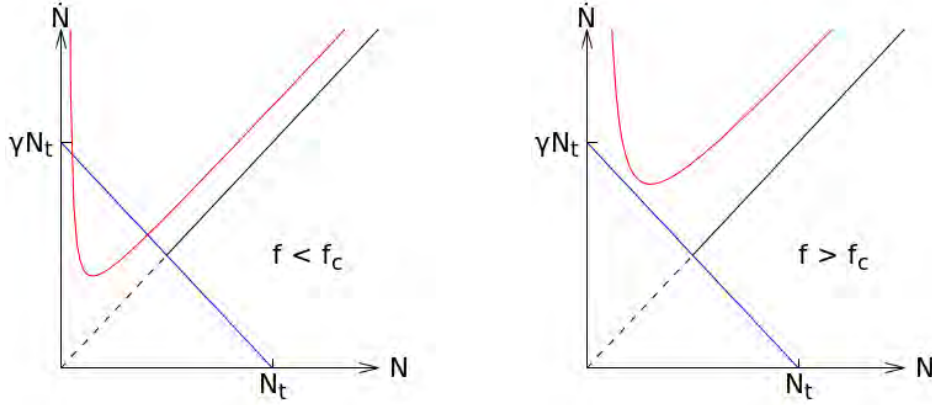
Example: Stability of adhesion cluster under constant force

We consider an adhesion cluster with bonds (receptor-ligand pairs) that can be either open or closed. If $N(t)$ represents the time-dependent number of closed bonds and N_t the total number of bonds, the number of open bonds is given as $N_t - N$. Two rates $k_{\text{off}}, k_{\text{on}}$ are used to describe the systems dynamics. In contrast to k_{on} , k_{off} depends on the acting force F . It can be written as $k_{\text{off}} = k_0 \cdot \exp(\frac{F}{F_0 \cdot N}) = k_0 \cdot \exp(\frac{f}{N})$. Furthermore using $\gamma = \frac{k_{\text{on}}}{k_0}$ and the dimensionless force $f = \frac{F}{F_0}$, the time-dependent number of bonds is given by

$$\begin{aligned} \frac{dN}{dt} &= k_{\text{on}} \cdot (N_t - N) - k_{\text{off}} \cdot N \\ &= k_{\text{on}} \cdot (N_t - N) - k_0 \cdot \exp(\frac{f}{N}) \cdot N. \end{aligned}$$

$$\Rightarrow \dot{N} = \frac{dN}{d\tau} = -N \cdot \exp(\frac{f}{N}) + \gamma \cdot (N_t - N)$$

in dimensionless time $\tau = k_0 \cdot t$. The graphical analysis shows the different cases for $f < f_c$ and $f > f_c$. The fixed points are given by $N \cdot \exp(\frac{f}{N}) = \gamma \cdot (N_t - N)$.



Below, the bifurcation point f_c is calculated using two equations.

$$N_c \cdot \exp(\frac{f_c}{N_c}) = \gamma \cdot (N_t - N_c) \quad (3.1.1)$$

$$N_c \cdot \exp(\frac{f_c}{N_c}) \left(1 - \frac{f_c}{N_c}\right) = \gamma \cdot N_c \quad (3.1.2)$$

$$\gamma = \frac{f_c}{N_c} \cdot \exp(\frac{f_c}{N_c}) \quad (3.1.3)$$

Equation (1) represents the fixed points. Dividing (2) by (1) results in

$$\left(1 - \frac{f_c}{N_c}\right) = -\frac{N_c}{N_t - N_c} \quad \Rightarrow \quad f_c = \frac{N_t N_c}{N_t - N_c} \quad \Rightarrow \quad \frac{f_c}{N_c} = \frac{f_c}{N_t} + 1$$

Using this, γ can be written as

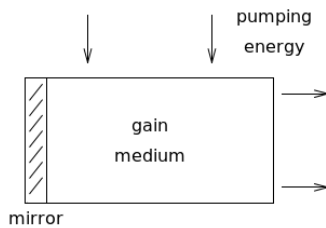
$$\gamma = \frac{f_c}{N_t} \cdot \exp\left(\frac{f_c}{N_t} + 1\right) \quad \Rightarrow \quad \frac{f_c}{N_t} \cdot \exp\left(\frac{f_c}{N_t}\right) = \frac{\gamma}{e} \quad \Rightarrow \quad \boxed{f_c = N_t \cdot \text{plog}\left(\frac{\gamma}{e}\right)}$$

. In the last step, the function plog is used, defined by $x \cdot \exp(x) = Q \Rightarrow x = \text{plog}(Q)$.

3.2 Transcritical bifurcation

The general form of a transcritical bifurcation $\dot{x} = r \cdot x - x^2$ leads to the fixed point $x^* = 0$ which exists for an arbitrary bifurcation parameter r and also represents the bifurcation point $r^c = 0$. The second fixed point $x^* = r$ is stable for $r > 0$ and unstable for $r < 0$. Depending on the application, not every fixed point is reasonable, e.g. when the population size is always positive.

A good example for a transcritical bifurcation is a laser. The rate of the photons in the laser $\dot{n}(t)$ is determined by the difference between gain and loss. Since the photons stimulate the atoms, the gain is proportional to both the number of photons in the laser $n(t)$ and the number of excited atoms $N(t)$. The gain coefficient is positive: $G > 0$. The loss of photons is determined by the rate constant $k > 0$.



$$\begin{aligned} \dot{n}(t) &= \text{gain} - \text{loss} \\ &= G \cdot n \cdot N - k \cdot n \end{aligned}$$

Introducing the maximal possible number of excited atoms N_0 , the number of excited atoms can be written as $N(t) = N_0 - \alpha \cdot n(t)$. Hence, the rate \dot{n} computes as

$$\dot{n}(t) = (GN_0 - k) \cdot n - G \cdot \alpha \cdot n^2.$$

Thus, the fixed points are $n_1^* = 0$ and $n_2^* = \frac{GN_0 - k}{\alpha G}$. Since n describes a particle number, demanding $n_2^* > 0$ is reasonable and leads to $N_0 > \frac{k}{G}$.

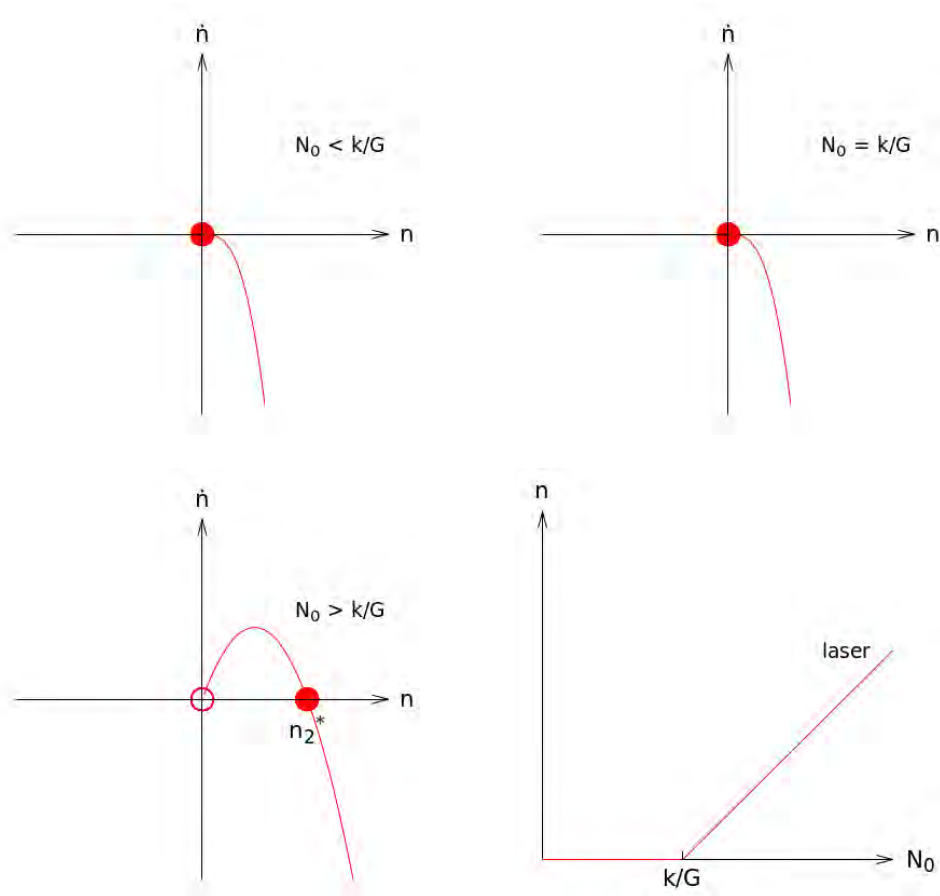
The fixed points stability analysis is done by evaluating

$$g'_N(n^*) = \frac{d\dot{n}}{dn}(n^*) = (GN_0 - k) - 2G\alpha n^*.$$

$$g'_n(n_1^*) = GN_0 - k = \begin{cases} < 0, & \text{for } N_0 < \frac{k}{G}, \text{ stable fixed point} \\ > 0, & \text{for } N_0 > \frac{k}{G}, \text{ unstable fixed point} \end{cases}$$

$$g'_n(n_2^*) = k - GN_0 < 0, \text{ since } N_0 > \frac{k}{G}, \text{ stable fixed point}$$

Obviously, $N_0 = \frac{k}{G}$ is a bifurcation point.



3.3 Pitchfork bifurcation

As the general form reads $\dot{x} = rx \pm x^3$ two different types exist: the *supercritical* and the *subcritical pitchfork bifurcation*.

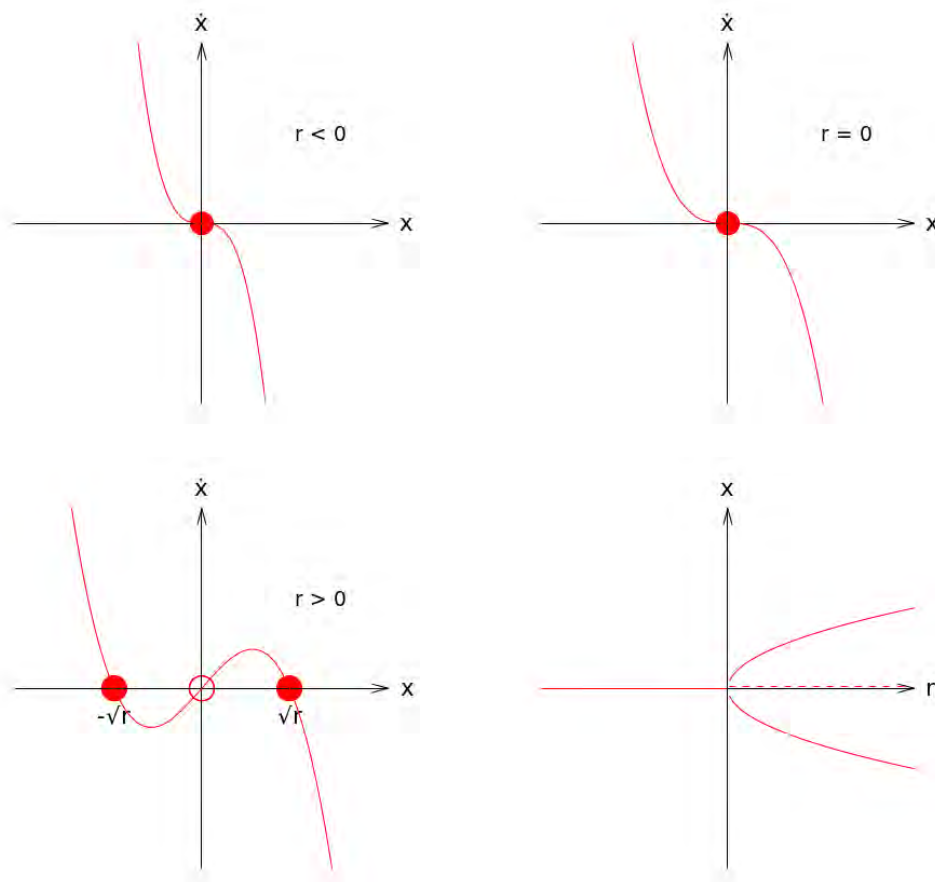
3.3.1 Supercritical pitchfork bifurcation

Considering firstly $f(x, r) = \dot{x} = rx - x^3$, the fixed points compute as $x_1^* = 0$ and $x_{2/3}^* = \pm\sqrt{r}$ if $r > 0$. The stability analysis yields

$$f'_x(x, r) = r - 3x^2.$$

$$f'_x(x_1^*) = r = \begin{cases} < 0, & \text{for } r < 0, \text{ stable fixed point} \\ > 0, & \text{for } r > 0, \text{ unstable fixed point} \end{cases}$$

$$f'_x(x_{2/3}^*) = -2r, \text{ stable fixed point since } x_{2/3}^* \text{ only exist for } r > 0$$



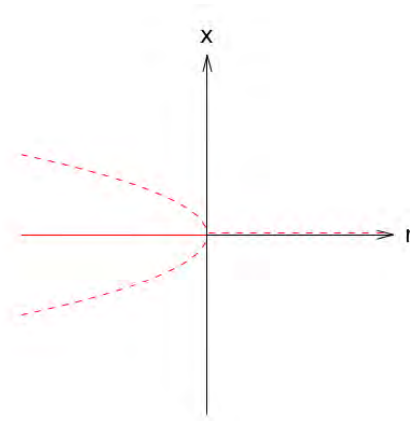
3.3.2 Subcritical pitchfork bifurcation

Now, $f(x, r) = \dot{x} = rx + x^3$. The fixed points are similar: $x_1^* = 0$ and $x_{2/3}^* = \pm\sqrt{-r}$ if $r < 0$. In this case, the properties are:

$$f'_x(x, r) = r + 3x^2.$$

$$f'_x(x_1^*) = r = \begin{cases} < 0, & \text{for } r < 0, \text{ stable fixed point} \\ > 0, & \text{for } r > 0, \text{ unstable fixed point} \end{cases}$$

$$f'_x(x_{2/3}^*) = -2r, \text{ unstable fixed point since } x_{2/3}^* \text{ only exist for } r < 0$$



So, the two types of pitchfork bifurcation differ in the second and third fixed point which are symmetrical in both cases. By now, the system is unstable. But it can be stabilized by using high order terms.

3.4 Influence of high order terms

In order to stabilize pitchfork bifurcations, a fifth order term is used. For instance, consider the following equation:

$$\dot{x} = rx + x^3 - x^5.$$

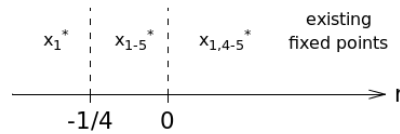
The fixed points are

$$x_1^* = 0$$

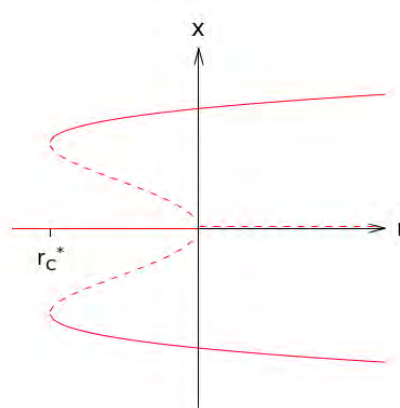
$$x_{2/3}^* = \pm \sqrt{\frac{1 + \sqrt{1 + 4r}}{2}}, \text{ exists for } 1 + 4r > 0$$

$$x_{4/5}^* = \pm \sqrt{\frac{1 - \sqrt{1 + 4r}}{2}}, \text{ exists for } -1 < 4r < 0$$

The existing fixed points in dependence of the bifurcation parameter r are shown in the next figure.



The bifurcation diagram is particularly interesting because there are different bifurcation types visible. The surrounding of $r = 0$ is characterized by a subcritical pitchfork bifurcation, whereas the transition of the unstable to the stable branch at r_c^* describes a saddle-node bifurcation.



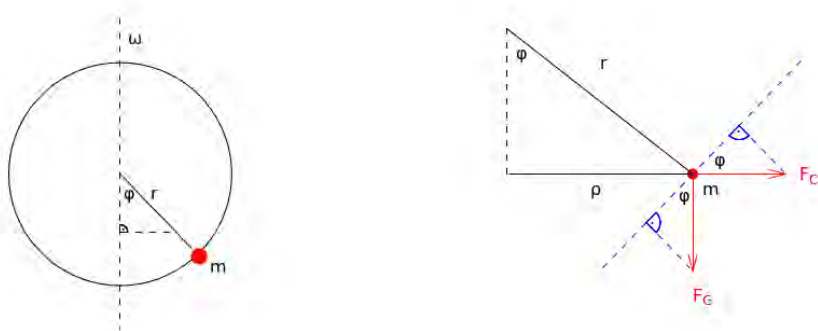
As well, a *hysteresis effect* is possible in this configuration. Starting at $r > r_c^*$, $x = 0$ and increasing r up to $r > 0$ leads to an unstable condition. A small perturbation results in a transition to a stable branch at same r . Decreasing r again, the system remains on the stable branch. This shows that the system does not come back to the original fixed point.

3.5 Summary of 1d bifurcations

The general form is $f(x, r) = \dot{x}$ and behaves as shown in the following table:

	normal form	$f(x^*)$	$f'_x(x^*, r_c)$	$f'_r(x^*, r_c)$	$f''_{xx}(x^*, r_c)$	$f''_{xr}(x^*, r_c)$	$f'''_{xxx}(x^*)$
saddle-node bifurcation	$\dot{x} = r + x^2$	0	0	$\neq 0$	$\neq 0$		
transcritical bifurcation	$\dot{x} = rx - x^2$	0	0	0	$\neq 0$	$\neq 0$	
pitchfork bifurcation	$\dot{x} = rx \pm x^3$	0	0	0	0	0	$\neq 0$

Example: Overdamped bead on a rotating hoop



The hoop is rotating around the axis with an angular velocity ω . The acting forces are the gravitational force F_G , the centrifugal force F_C and a friction force F_R which describes the system in a fluid. They are projected on the ϕ -plane.

$$\begin{aligned}
F_G &= m \cdot g && \rightarrow mg \cdot \sin(\phi) \\
F_C &= m \cdot \rho \cdot \omega^2 && \rightarrow m\rho\omega^2 \cdot \cos(\phi) \\
F_R &= -b\dot{\phi}
\end{aligned}$$

Using $\rho = r \cdot \sin(\phi)$, the total acting force yields

$$F = m \cdot r\ddot{\phi} = -b \cdot \dot{\phi} - mg \cdot \sin(\phi) + mr\omega^2 \cdot \sin(\phi) \cos(\phi).$$

In order to receive a first order equation, the term $m \cdot r\ddot{\phi}$ shall be neglected. The time $\tau = \frac{t}{T}$ with the timescale T is introduced. In a second step, the equation is reformulated dimensionless by dividing by the gravitational force F_G .

$$\begin{aligned}
\left(\frac{m\tau}{T^2}\right)^2 \frac{d^2\phi}{d\tau^2} &= -\frac{b}{T} \frac{d\phi}{d\tau} - mg \cdot \sin(\phi) + mr\omega^2 \cdot \sin(\phi) \cos(\phi) \\
\left(\frac{\tau}{gT^2}\right)^2 \frac{d^2\phi}{d\tau^2} &= -\frac{b}{Tmg} \frac{d\phi}{d\tau} - \sin(\phi) + \frac{r\omega^2}{g} \cdot \sin(\phi) \cos(\phi)
\end{aligned}$$

How to define T so that $\epsilon^2 := \left(\frac{\tau}{gT^2}\right)^2$ is negligible?

Choosing the prefactor of the friction force $-\frac{b}{Tmg}$ to be of order 1, T is defined to be $T = \frac{b}{mg}$. With this, ϵ is negligible if $\epsilon = \frac{\tau}{gT^2} = \frac{m^2g\tau}{g^2} \ll 1$, so if the inertia is much smaller than the friction.

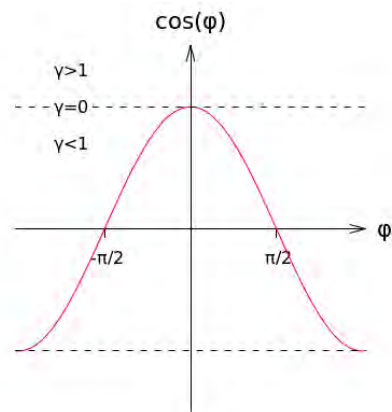
Set $\epsilon = 0$ from now on and introduce $\gamma := \frac{r\omega^2}{g}$. The equation computes as

$$\frac{d\phi}{d\tau} = \sin(\phi) (\gamma \cdot \cos(\phi) - 1).$$

The applied procedure has reduced the number of parameters from five to two: ϵ and γ . But setting $\epsilon = 0$ transforms the equation to dimension one. So, only one initial condition can be considered. Thus, the behavior of the system "at the very beginning" is neglected. After that, the system behaves as if it was of the order of 1.

The fixed points result from $\sin(\phi) = 0$ and $\cos(\phi) - \frac{1}{\gamma} = 0$. Therefore, the number of fixed points depends on γ :

For $|\gamma| > 1$ there are only the fixed points due to $\sin(\phi) = 0$. For the bifurcation point $|\gamma| = 1$, one additional fixed point exists for each period of ϕ and for $|\gamma| < 1$, there are actually two.



Chapter 4

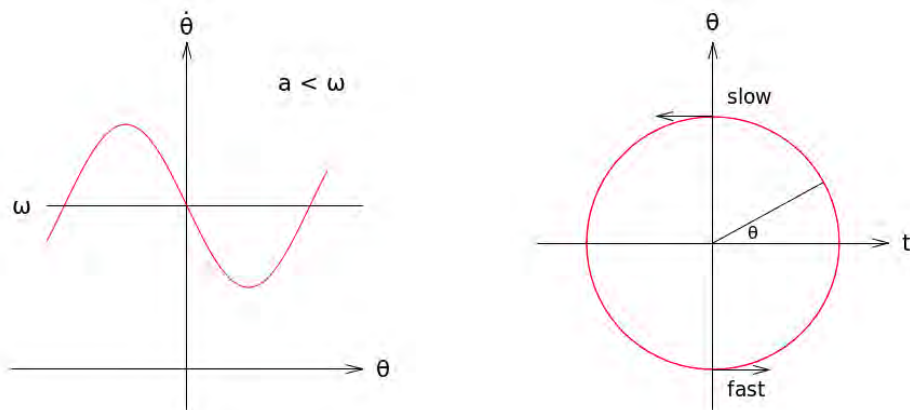
Flow on a circle

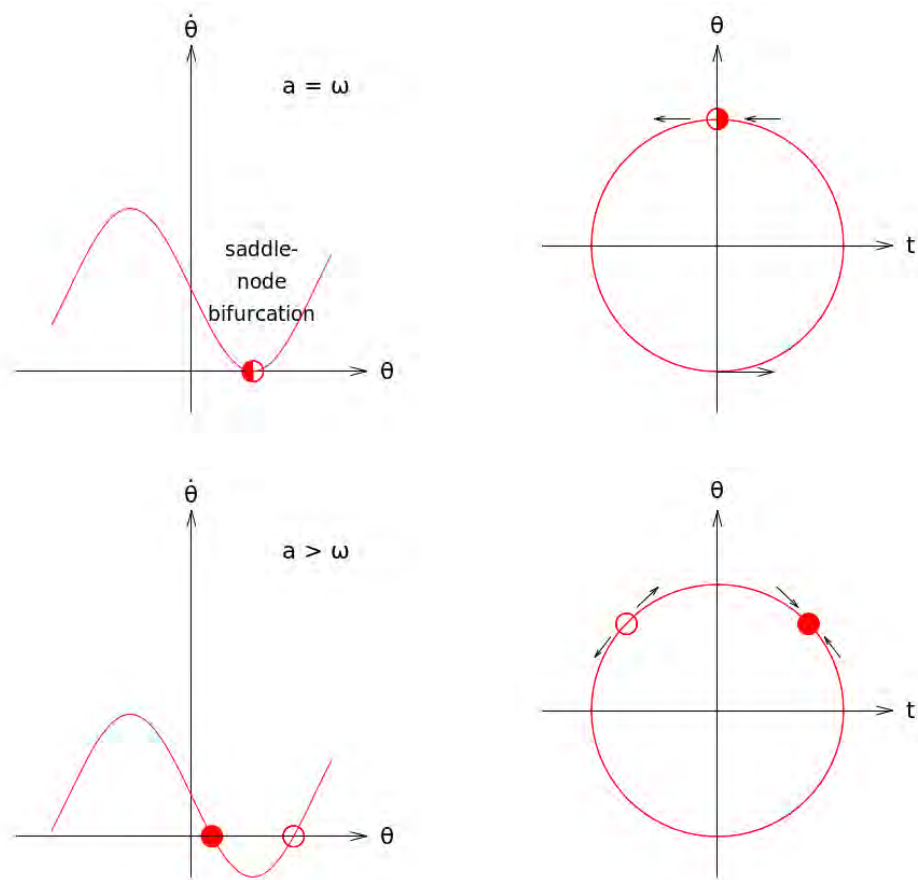
So far, we considered linear systems $\dot{x} = f(x)$ and visualized their dynamics as flow on a line. Now, we are taking into account periodic behavior using the differential equation $\dot{\theta} = f(\theta)$. Then, $f(\theta + 2\pi) = f(\theta)$. This corresponds to a vector field on the circle.

The simplest case is a constant velocity $\dot{\theta} = f(\theta) = \text{const} = \omega$ leading to an oscillation with period $T = \frac{2\pi}{\omega}$ but without amplitude, $\theta(t) = \omega \cdot t + \omega_0$.

The simplest non-trivial case is $\dot{\theta} = \omega - a \cdot \sin(\theta)$. It has various applications in different branches of science: e.g. Josephson junctions, electronics, biological oscillations, mechanics, etc.

a is a bifurcation parameter ($a > 0$). Depending on its relation to ω , the following phase portraits (lhs) and corresponding flow diagrams (rhs) exist.

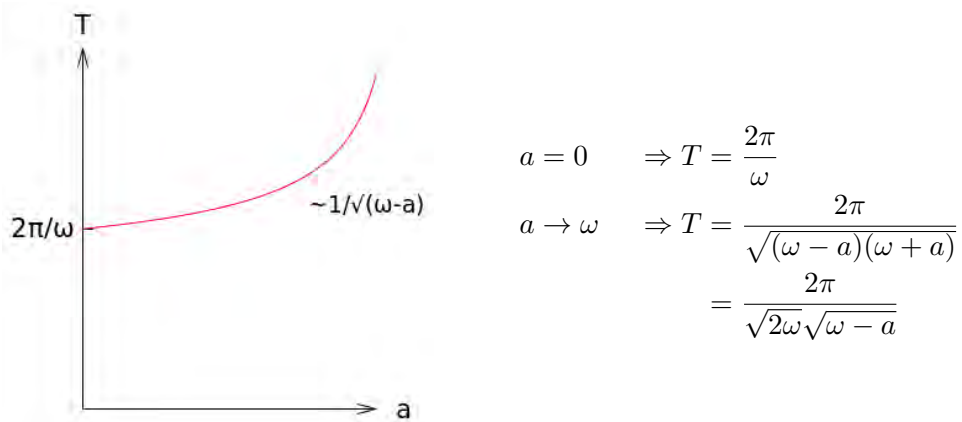




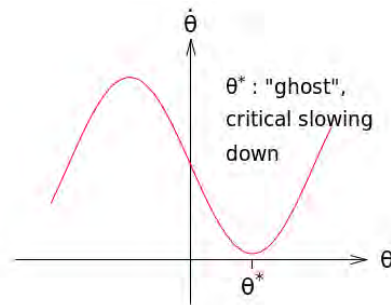
What is the oscillation period T ?

$$T = \int dt = \int_0^{2\pi} \frac{dt}{d\theta} d\theta = \int_0^{2\pi} \frac{1}{\frac{d\theta}{dt}} d\theta = \int_0^{2\pi} \frac{1}{\omega - a \cdot \sin(\theta)} d\theta = \frac{2\pi}{\sqrt{\omega^2 - a^2}}$$

Obviously, the oscillation period depends on a .



The scaling is generic for a saddle-node bifurcation.



A Taylor expansion around the critical value $\theta^* = \frac{\pi}{2}$ by introducing $\Phi = \theta - \theta^*$

$$\begin{aligned}
 \dot{\Phi} &= \omega - a \cdot \sin\left(\Phi + \frac{\pi}{2}\right) \\
 &= \omega - a \cdot \cos(\Phi) \\
 &\approx \omega - a + \frac{1}{2}a \cdot \Phi^2
 \end{aligned}$$

results in the normal form of saddle-node bifurcations:

$$\begin{aligned}
 x &:= \left(\frac{a}{2}\right)^{1/2} \Phi \\
 r &:= \omega - a
 \end{aligned}$$

$$\Rightarrow \left(\frac{2}{a}\right)^{1/2} \dot{x} = r + x^2.$$

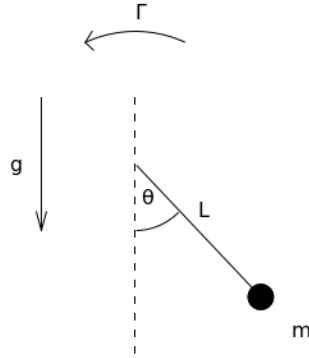
Most of the time will be spent close to θ^* .

$$T = \int dt = \int_{-\infty}^{\infty} \frac{dt}{dx} dx = \left(\frac{2}{a}\right)^{1/2} \int dr \frac{1}{r+x^2} = \left(\frac{2}{a}\right)^{1/2} \frac{\pi}{\sqrt{r}} = \left(\frac{2}{\omega}\right)^{1/2} \frac{\pi}{\sqrt{\omega-a}}$$

This is the same result as above. Therefore, extending the integration boundaries to infinity is indeed not a problem.

Examples

1. Driven overdamped pendulum $b\dot{\theta} + mgL \sin(\theta) = \Gamma$



Dividing by mgL leads to the dimensionless equation

$$\underbrace{\frac{b}{mgL}}_{=\tau_0} \dot{\theta} + \sin(\theta) = \frac{\Gamma}{mgL} =: \gamma.$$

The bifurcation parameter γ is the quotient of the applied torque Γ to the maximum gravitational torque. Having also introduced the dimensionless time $\tau_0 = \frac{t}{\tau}$ the system is described by the equation

$$\dot{\theta} = \frac{d\theta}{d\tau} = \gamma - \sin(\theta).$$

At $\gamma = 1$ the pendulum stops its motion. For $\gamma < 1$ the external torque is too weak to drive the pendulum around.

2. Firefly synchronization

Identify $\theta = 0$ with the emission of the flash.

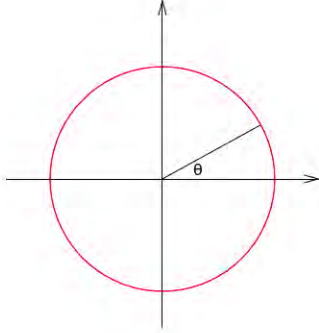
Without external stimulus, each firefly has $\dot{\theta} = \omega$. Now, consider a periodic stimulus with phase Ξ which satisfies

$$\dot{\Xi} = \Omega. \quad (4.0.1)$$

The basic model to simulate the firefly's reaction to the stimulus is given by

$$\dot{\theta} = \omega + A \cdot \sin(\Xi - \theta) \quad (4.0.2)$$

with the resetting or coupling strength A .

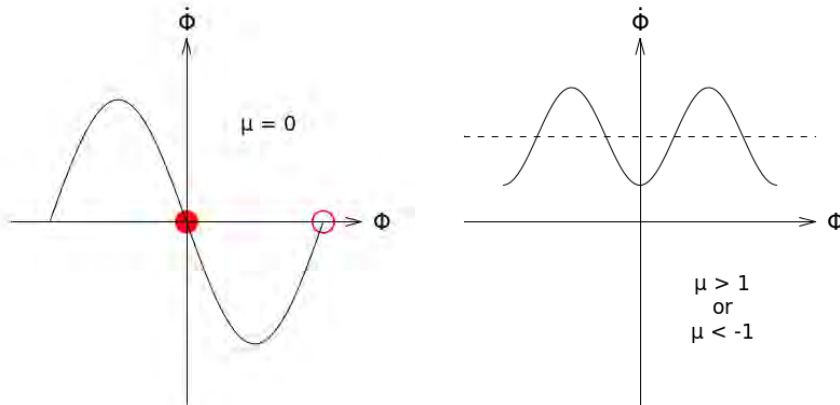


The last equation can be expressed using the phase difference $\Phi = \Xi - \theta$. Subtracting (4.0.2) from (4.0.1) leads to $\dot{\Phi} = \Omega - \omega - A \cdot \sin(\Phi)$. Defining furthermore $\mu := \frac{\Omega - \omega}{A}$ and $\tau = A \cdot t$ the final equation reads

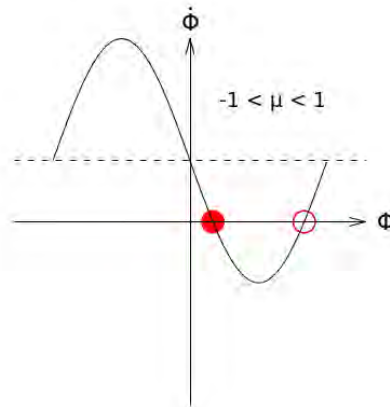
$$\dot{\Phi} = \frac{d\Phi}{d\tau} = \mu - \sin(\Phi)$$

.

This leads to the following phase space diagrams:



For $\mu = 0$, there is a perfect synchrony at $\Phi = 0$. If $\mu > 1$ (or $\mu < -1$) there aren't any stable fixed points. So, there is no synchrony but a *phase drift*. The oscillation occurs with $T = \frac{2\pi}{\sqrt{(\Omega - \omega)^2 - A^2}}$.



The interval $-1 < \mu < 1$ is called the *range of entrainment*. There is synchrony at the stable fixed point but with a phaselag. The stimulus entrains the oscillation with a frequency Ω if $\omega - A < \Omega < \omega + A$. This is called *phase locking*.

In our example, now all fireflies flash in synchrony, but with a possible lag to the external stimulus (e.g. a flash light).

Chapter 5

Flow in linear 2d systems

5.1 General remarks

In 2d, the variety of dynamical behavior is much larger than in 1d.

As a first step, we look at linear systems in two dimensions. Then, a complete classification is possible and starts from

$$\dot{x} = A \cdot \vec{x} = \begin{pmatrix} a & b \\ c & d \end{pmatrix} \begin{pmatrix} x_1 \\ x_2 \end{pmatrix}.$$

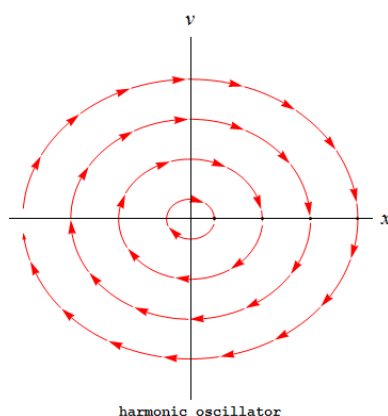
In general, if $\vec{x}_1(t)$ and $\vec{x}_2(t)$ are solutions of the equation, so is $c_1 \cdot \vec{x}_1 + c_2 \cdot \vec{x}_2$. In addition, $\vec{x} = 0$ is always a solution.

Graphical analysis can be done by drawing and analyzing the "phase plane" (x_1, x_2) .

Examples

1. **Harmonic oscillator:** $m\ddot{x} + kx = 0$

Defining the frequency $\omega_0 = \sqrt{\frac{k}{m}}$ and choosing $x_1 = x$, $x_2 = \dot{x} = v$ as done in section 1 the matrix is $A = \begin{pmatrix} 0 & 1 \\ -\omega_0^2 & 0 \end{pmatrix}$.



Why are the trajectories ellipses?

$$\begin{aligned}\frac{\dot{x}}{\dot{v}} &= \frac{v}{-\omega_0^2 \cdot x} \\ \Rightarrow -\omega_0^2 \cdot x \, dx &= v \, dv \\ \Rightarrow \boxed{-\omega_0^2 \cdot x^2 - v^2} &= \text{const}\end{aligned}$$

This corresponds to energy conservation:

$$\frac{1}{2}kx^2 + \frac{1}{2}mv^2 = \text{const.}$$

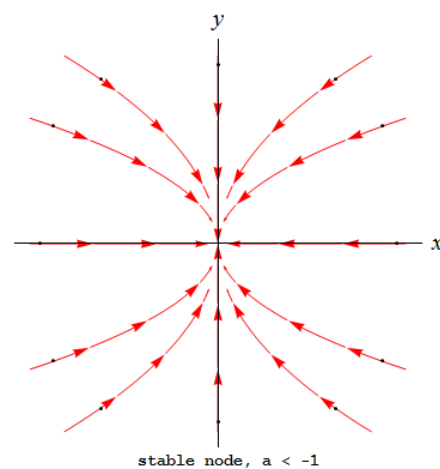
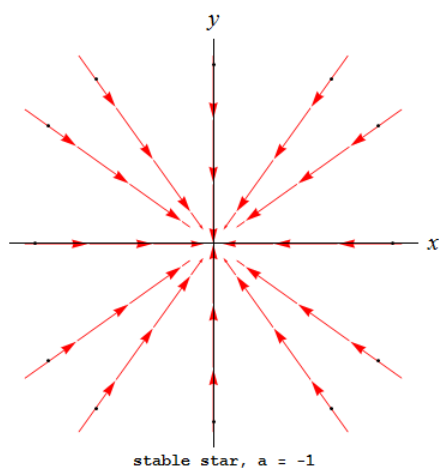
2. **A linear 2d system without oscillation:** $\begin{pmatrix} \dot{x} \\ \dot{y} \end{pmatrix} = \begin{pmatrix} a & 0 \\ 0 & -1 \end{pmatrix} \begin{pmatrix} x \\ y \end{pmatrix}$

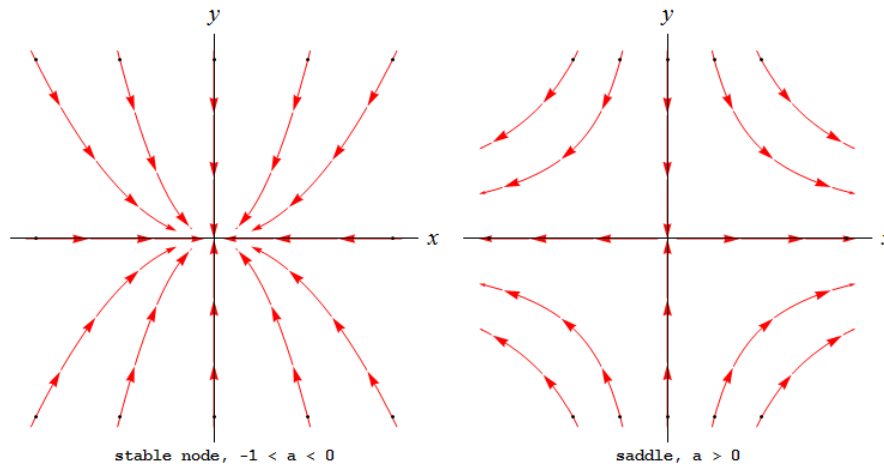
For the given matrix $A = \begin{pmatrix} a & 0 \\ 0 & -1 \end{pmatrix}$, the two equations are uncoupled. They can be separately solved using an exponential ansatz.

$$\begin{aligned}\dot{x} &= a \cdot x \\ \dot{y} &= -y\end{aligned}$$

$$\begin{aligned}x(t) &= x_0 \cdot \exp(a \cdot t) \\ y(t) &= y_0 \cdot \exp(-t)\end{aligned}$$

The phase portraits differ depending on a .





5.2 Phase plane flow for linear systems

Consider the linear case

$$\dot{\vec{x}} = A \cdot \vec{x} = \begin{pmatrix} a & b \\ c & d \end{pmatrix} \vec{x}.$$

Our analysis is based on the two eigenvalues λ_1, λ_2 of $A = \begin{pmatrix} a & b \\ c & d \end{pmatrix}$. They are calculated using the characteristic equation $A \cdot \vec{v} = \lambda \cdot \vec{v}$.

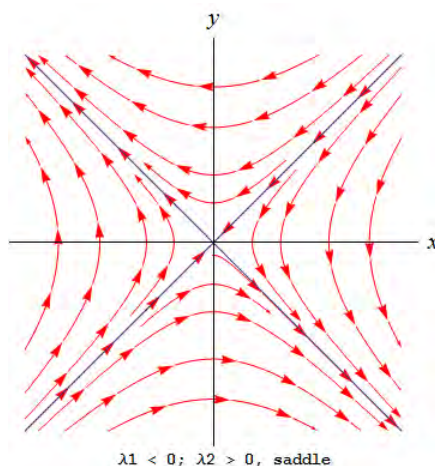
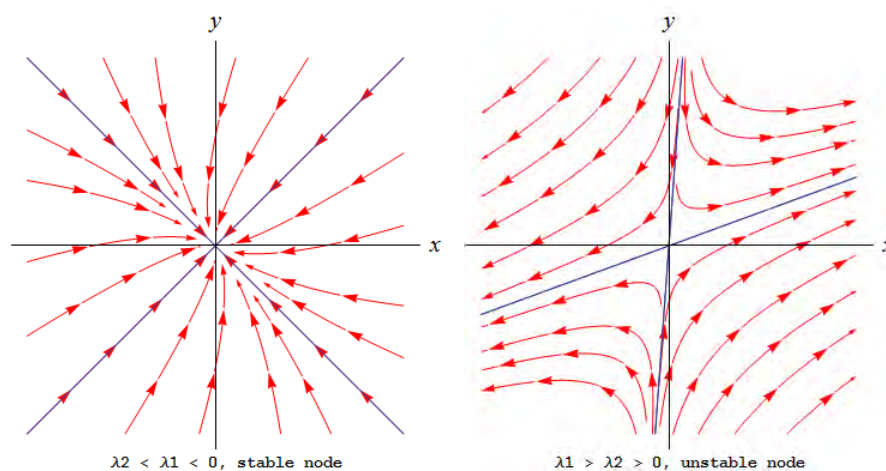
$$\begin{aligned} 0 &\stackrel{!}{=} \det \begin{pmatrix} a - \lambda & b \\ c & d - \lambda \end{pmatrix} = \lambda^2 - \tau\lambda - \Delta \\ &= (\lambda - \lambda_1)(\lambda - \lambda_2) \\ \Rightarrow \lambda_{1/2} &= \frac{\tau \pm \sqrt{\tau^2 - 4\Delta}}{2} \end{aligned}$$

with $\tau = a + d = \text{tr } A = \lambda_1 + \lambda_2$ and $\Delta = ad - cb = \det A = \lambda_1\lambda_2$.

In general, the eigenvalues are complex numbers depending on the trace τ and the determinant Δ of A . If the eigenvalues are different $\lambda_1 \neq \lambda_2$, the eigenvectors $\vec{v}_{1/2}$ are linearly independent. Hence, the characteristics of A determines the phase plane flow as shown below. The time-dependent eigenvectors can be calculated using $\vec{x}_{1/2}(t) = \exp(\lambda_{1/2} \cdot t) \cdot \vec{v}_{1/2}$.

We now completely enumerate all possible cases.

1. Real eigenvalues

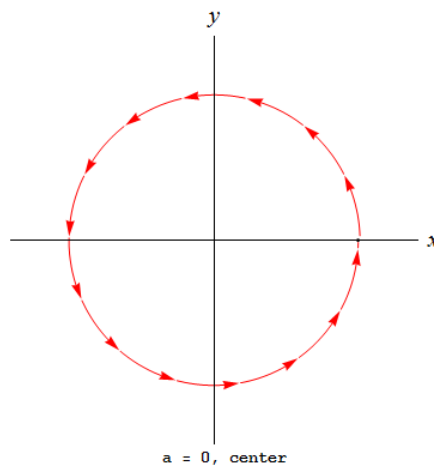
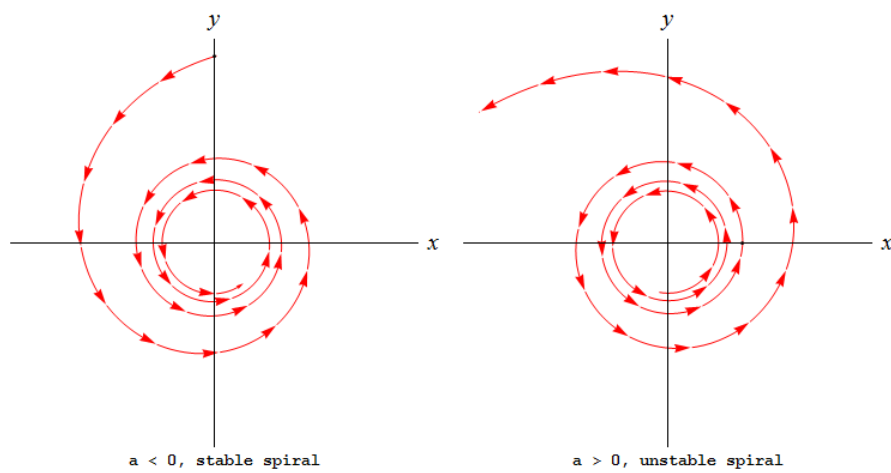


2. Complex eigenvalues

If the discriminant is smaller than zero, $\tau^2 - 4 \cdot \Delta < 0$, the eigenvalues are complex. Defining $\omega = \frac{1}{2} \sqrt{-(\tau^2 - 4 \cdot \Delta)}$, the eigenvalues read $\lambda_{1/2} = \frac{\tau}{2} \pm i\omega$. The general solution can be decomposed in the directions of the eigenvalues.

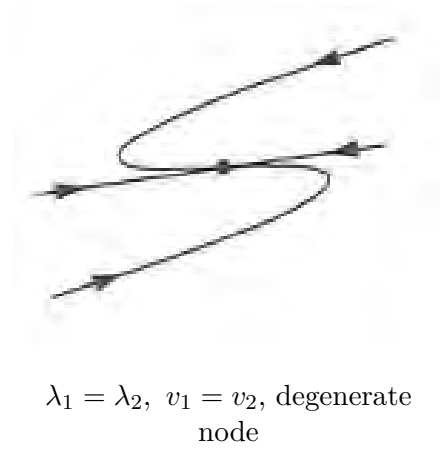
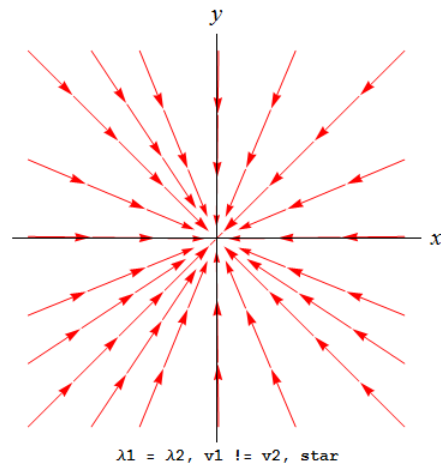
$$\vec{x}(t) = (c_1 \vec{v}_1 \exp(i\omega t) + c_2 \vec{v}_2 \exp(-i\omega t)) \cdot \exp(\alpha t)$$

Now, there are oscillations in the system. If $\alpha < 0$ the amplitude is decaying. In contrast, if $\alpha > 0$ it is exploding. Only if $\alpha = 0$ the amplitude is constant. In this case, the eigenvalues are purely imaginary. It is the boundary between stability and instability.



3. Equal eigenvalues

The eigenvalues are equal if the discriminant is zero $\tau^2 - 4 \cdot \Delta = 0$. Then, the eigenvectors exhibit the same velocity. They can either be different or the same. In both cases, stable and unstable phase portraits exist. As an example, the stable ones are plotted.

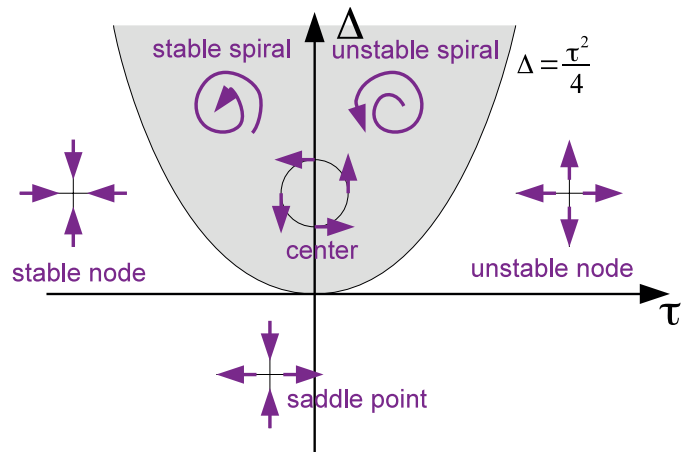


4. At least one eigenvalue is zero

In this case, the phase portrait is a line or plane of fixed points.

Summary in one scheme

Saddles, nodes and spirals are the major types of fixed points.



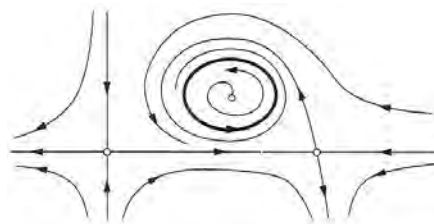
Chapter 6

Flow in non-linear 2d systems

Non-linear systems show a much larger variety of flow behavior.

$$\dot{x} = \begin{pmatrix} f_1(x) \\ f_2(x) \end{pmatrix}$$

Example

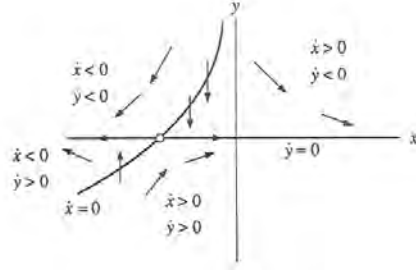


Recipe for phase space analysis:

1. Identify nullclines: lines with $\dot{x} = 0$ or $\dot{y} = 0$
2. Identify fixed points: intersections of nullclines
3. Linear stability analysis around fixed points

Example $\dot{x} = x + \exp(-y), \quad \dot{y} = -y$

The phase portrait shows four different regions varying in the sign of \dot{x} and \dot{y} . At $(-1,0)$, there is a saddle. Having drawn the nullclines it is easy to compute the remaining flow behavior.



Linear stability analysis:

At a fixed point (x^*, y^*) , we look at small deviations $u = x - x^*$ and $v = y - y^*$ using Cartesian coordinates. The derivatives are approximated in a Taylor expansion up to first order.

$$\begin{aligned} \dot{u} &= \dot{x} = f_1(x^* + u, y^* + v) \\ &= f_1(x^*, y^*) + \frac{\partial f_1}{\partial x} \cdot u + \frac{\partial f_1}{\partial y} \cdot v + \mathcal{O}(u^2, v^2, \dots) \\ \dot{v} &= \dot{y} = f_2(x^* + u, y^* + v) \\ &= f_2(x^*, y^*) + \frac{\partial f_2}{\partial x} \cdot u + \frac{\partial f_2}{\partial y} \cdot v + \mathcal{O}(u^2, v^2, \dots) \end{aligned}$$

Approximated up to first order, this can also be written as matrix equation.

$$\begin{pmatrix} \dot{u} \\ \dot{v} \end{pmatrix} = \underbrace{\begin{pmatrix} \partial_x f_1 & \partial_y f_1 \\ \partial_x f_2 & \partial_y f_2 \end{pmatrix}}_{=A} \begin{pmatrix} u \\ v \end{pmatrix}$$

A is the Jacobian at the fixed point. Calculating the eigenvalues of A , linear stability analysis can be performed. This works well for saddles, nodes and spirals. But it does not always work for borderline cases such as centers, stars, lines and planes of fixed points or degenerate nodes as shown in the following example.

Example: Rabbits and sheep

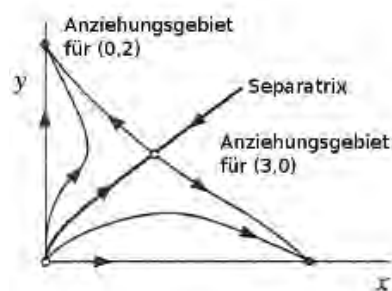
Consider the Lotka-Volterra model for two competing species x, y . The variables x and y name the population size of rabbits and sheep, respectively.

The rabbit population exhibits a faster logistic growth than the sheep population. As the sheep compete for grass with the rabbits, the growth rate of the rabbits \dot{x} decreases if more sheep exist while the sheep suffer only little under more rabbits.

$$\begin{aligned}\dot{x} &= x(3 - x - 2y) \\ \dot{y} &= y(2 - y - x)\end{aligned}$$

The Jacobian computes as $A = \begin{pmatrix} 3 - 2x - 2y & -2x \\ -y & 2 - 2y - x \end{pmatrix}$. The character of the four fixed points is different.

fixed point	(0,0)	(0,2)	(3,0)	(1,1)
A	$\begin{pmatrix} 3 & 0 \\ 0 & 2 \end{pmatrix}$	$\begin{pmatrix} -1 & 0 \\ -2 & -2 \end{pmatrix}$	$\begin{pmatrix} -3 & -6 \\ 0 & -1 \end{pmatrix}$	$\begin{pmatrix} -1 & -2 \\ -1 & -1 \end{pmatrix}$
τ	5	-3	-4	-2
Δ	6	2	4	-1
λ_1	3	-1	-2	$\sqrt{2} - 1$
λ_2	2	-2	-2	$-(\sqrt{2} - 1)$
classification	unstable node	stable node	stable node	saddle



Example: Pathological example

$$\begin{aligned}\dot{x} &= -y + ax(x^2 + y^2) \\ \dot{y} &= x + ay(x^2 + y^2)\end{aligned}$$

Obviously, $(x^*, y^*) = (0, 0)$ is a fixed point. In order to calculate the Jacobian, only the linear terms have to be considered.

$$A = \begin{pmatrix} 0 & -1 \\ 1 & 0 \end{pmatrix} \quad \Rightarrow \quad \tau = 0; \quad \Delta = 1; \quad \lambda_{1/2} = \pm i$$

In linear approximation, the fixed point is a center.

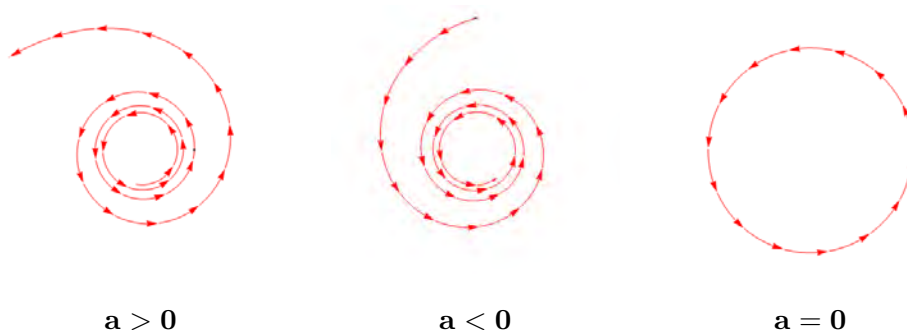
But this is not true for the non-linear case. To analyze this in more detail, we switch to polar coordinates $x = r \cdot \cos \theta$, $y = r \cdot \sin \theta$ and derive the equation of motion for r

$$\begin{aligned}r^2 &= x^2 + y^2 \\ r \cdot \dot{r} &= x \cdot \dot{x} + y \cdot \dot{y} = x(-y + axr^2) + y(x + ayr^2) = a \cdot r^4 \\ \Rightarrow \quad \dot{r} &= a \cdot r^3\end{aligned}$$

and θ :

$$\begin{aligned}\theta &= \arctan\left(\frac{y}{x}\right) \\ \Rightarrow \quad \dot{\theta} &= \frac{1}{1 + \left(\frac{y}{x}\right)^2} \cdot \frac{x\dot{y} - \dot{x}y}{x^2} = \dots = 1.\end{aligned}$$

Hence, the angular velocity $\dot{\theta}$ is constant. a is the important parameter. The situation is similar to flow on a circle, yet the radius as dynamic variable can either explode or decay.



A center occurs only for $a = 0$. But linear stability analysis predicted this for all values of a . Instead, the typical case is a spiral.

We next have a brief look at two different types of special situations: conservative (e.g. earth orbiting around the sun) and reversible systems (systems with time-reversal). These cases are sufficiently restrictive such that general rules follow that make calculations easier.

1. Conservative systems

In a conservative system, the acting force F can be derived for a potential V . For example, in 1d we have:

$$m \cdot \ddot{x} = F(x) = -\frac{dV}{dx}.$$

Multiplying with the velocity \dot{x} leads to

$$\begin{aligned} \frac{m}{2} \frac{d}{dt}(\dot{x}^2) &= -\frac{dV}{dt} \\ \Rightarrow \frac{d}{dt} \underbrace{\left(\frac{1}{2}m\dot{x}^2 + V\right)}_{=E} &= 0. \end{aligned}$$

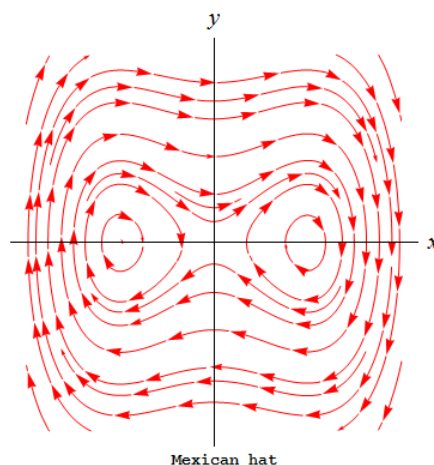
There exists a quantity E which is constant along trajectories (but not in an open set in \vec{x}). This corresponds to energy conservation.

Theorem: In a conservative system, an attractive fixed point cannot exist.

Proof: In such a case, there would be a basin of attraction and thus E could not be constant in a nontrivial way.

Example: Mexican hat $V(x) = -\frac{1}{2}x^2 + \frac{1}{4}x^4$

The second derivative is $\ddot{x} = x - x^3$. Three fixed points exist: $(0,0)$, $(1,0)$ and $(-1,0)$. Applying a simple trick $\dot{x} = y$ and $\dot{y} = x - x^3$ the phase portrait can be drawn.



Example: Hamiltonian system $H(q, p)$

It is $\dot{q} = \frac{\partial H}{\partial p}$ and $\dot{p} = -\frac{\partial H}{\partial q}$. From this, energy conservation simply follows:

$$\dot{H} = \partial_p H \cdot \dot{p} + \partial_q H \cdot \dot{q} = 0.$$

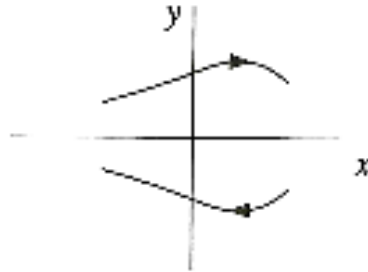
We know from the theorem that there are no attractive fixed points in the system. Instead, a typical fixed point is a center and thus often oscillations occur in the system.

2. Reversible systems

Time reversal symmetry is more general than energy conservation. Reversible, non-conservative systems occur e.g. fluid flow, laser, superconductors, etc.

Mechanical systems without damping are invariant under $t \rightarrow -t$. Consider in 1d, $m \cdot \ddot{x} = F(x)$, thus the force is time-independent. This is time-independent because of the second derivative. We introduce the velocity

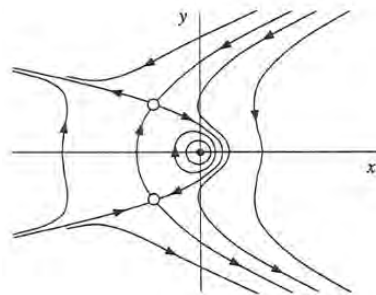
$$v = \dot{x} \quad \Rightarrow \quad \dot{v} = \frac{1}{m} F(x).$$



Both $(x(t), v(t))$ and $(x(-t), -v(-t))$ are solutions of the system in this framework. In general, there is a twin for each trajectory. Note the similarity to centers, which have trajectories that have merged at the ends.

Examples:

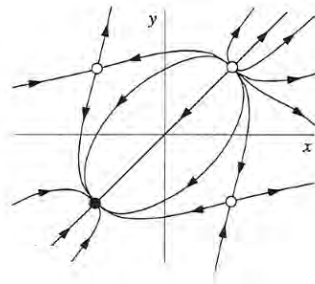
(a) $\dot{x} = y - y^3 \quad \dot{y} = -x - y^2$



The system is invariant under $t \rightarrow -t$ and $y \rightarrow -y$. There are three fixed points: two saddles and a center.

There is mirror symmetry around the x -axis in regard to the flow lines (but not the flow vectors).

(b) $\dot{x} = -2 \cos(x) - \cos(y) \quad \dot{y} = -2 \cos(y) - \cos(x)$



The system is invariant under $t \rightarrow -t$, $x \rightarrow -x$ and $y \rightarrow -y$.

Four fixed points exist $(x^*, y^*) = (\pm \frac{\pi}{2}, \pm \frac{\pi}{2})$: two saddles, one stable node and one unstable node. Since the stable node is an attractive fixed point, this is not a conservative system.

Now, there is mirror symmetry around the bisector.

Numerical integration of ODE's

Several numerical integration methods for ODE's exist, differing in their accuracy. They are based on a Taylor expansion up to a certain order. In the following, we have a closer look at three different methods.

1. Euler method:

The time t is discretized. Starting at t_n , the next step is computed multiplying the velocity at t_n with the time step Δt . This corresponds to a first order Taylor expansion

$$x_{n+1} = x_n + f(x_n)\Delta t + \mathcal{O}(\Delta t^2).$$

Since this accuracy is not very good, higher order methods are often applied.

2. Runge-Kutta methods:

The Runge-Kutta methods combine several Euler-style steps. A second order accuracy is achieved by using the mid-point velocity of the integration step.

$$\begin{aligned} k_1 &= f(x_n)\Delta t, & k_2 &= f\left(x_n + \frac{k_1}{2}\right)\Delta t \\ \Rightarrow x_{n+1} &= x_n + k_2 + \mathcal{O}(\Delta t^3) \end{aligned}$$

We see that two function evaluations are needed. In an analogous manner, we maintain fourth order accuracy:

$$\begin{aligned} k_1 &= f(x_n)\Delta t, & k_2 &= f\left(x_n + \frac{k_1}{2}\right)\Delta t, \\ k_3 &= f\left(x_n + \frac{k_2}{2}\right)\Delta t, & k_4 &= f\left(x_n + \frac{k_3}{2}\right)\Delta t, \end{aligned}$$

$$\Rightarrow x_{n+1} = x_n + \frac{1}{6}(k_1 + 2k_2 + 2k_3 + k_4) + \mathcal{O}(\Delta t^5)$$

Obviously, this requires four function evaluations. It is the a very good choice if the number of evaluations is not essential. To realize this, one standard choice is Matlab ODE 45 (see also on the web page).

3. Störmer-Verlet methods: ("leaping frog")

Störmer-Verlet methods are especially suited for Hamiltonian systems, e.g. molecular dynamics. The simplest version is:

$$\ddot{x} = f(x) \quad \Rightarrow \quad f(x_n) = \frac{x_{n+1} + x_{n-1} - 2x_n}{\Delta t^2}$$

$$x_{n+1} = 2x_n - x_{n-1} + f(x_n)\Delta t^2$$

We now rewrite this as 2d system. We define the velocity $v = \dot{x}$ and discretize the function $f(x) = \dot{v}$. For each integration step, the position is updated for a full time step and the velocity half a time step. The resulting equations are:

$$\begin{aligned} v_{n+1/2} &= v_n + \frac{\Delta t}{2} f(x_n) \\ x_{n+1} &= x_n + v_{n+1/2} \Delta t \\ v_{n+1} &= v_{n+1/2} + \frac{\Delta t}{2} f(x_{n+1}) \end{aligned}$$

This procedure is called *leaping frog* because we have staggered jumps.

Chapter 7

Oscillations in 2d

In contrast to linear systems, non-linear ones allow for *limit cycles*. These are isolated closed trajectories in the phase plane. They cannot exist in linear systems because with $x(t)$ also $cx(t)$ is a trajectory, thus closed orbits cannot exist in isolation.

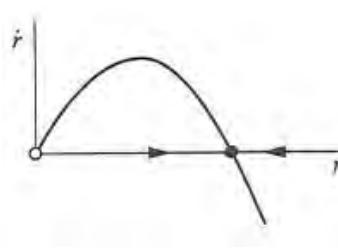
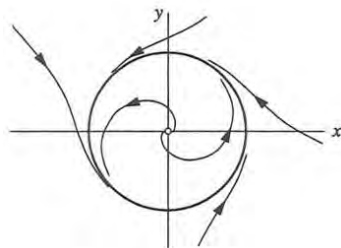
Poincare-Bendixson theorem:

If R is a closed, bounded subset of the plane without any fixed point, and if there is a trajectory that is confined in R , then R contains a closed orbit.

The second condition is satisfied if a *trapping region* R exists. To prove that a stable limit cycle exists, we have to show that a trapping region exists without a fixed point inside. The Poincare-Bendixson theorem also implies that there is no chaos in two dimensions; in three dimensions and higher, the Poincare-Bendixson theorem does not apply and the trajectory could wander around in a constrained space without settling into a closed orbit.

Examples:

1. $\dot{r} = r(1 - r^2), \quad \dot{\theta} = 1$



In Cartesian coordinates:

$$\begin{aligned}\dot{x} &= (1 - x^2 - y^2)x - y \\ \dot{y} &= (1 - x^2 - y^2)y - x.\end{aligned}$$

2. $\dot{\mathbf{r}} = \mathbf{r}(1 - \mathbf{r}^2) + \mu\mathbf{r} \cos(\theta), \quad \dot{\theta} = 1$

In this more complicated example, for which values of $\mu \geq 0$ does a stable limit cycle exist?

The trapping region can be determined for the given example by constructing minimum and maximum radius r_{min} , r_{max} and demanding an increasing and decreasing flow, respectively.

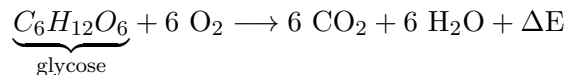
$$\begin{aligned}r_{min} : \dot{r} \geq r(1 - r^2) - \mu r > 0 &\Rightarrow r_{min} < \sqrt{1 - \mu} \\ r_{max} : \dot{r} \leq r(1 - r^2) + \mu r < 0 &\Rightarrow r_{max} > \sqrt{1 + \mu}\end{aligned}$$

Since $\sqrt{1 + \mu}$ is always real for $\mu \geq 0$, the only restriction for the trapping region comes from r_{min} : $0 \leq \mu < 1$. Due to the Poincaré-Bendixson theorem, we have a stable limit cycle for these values of μ .

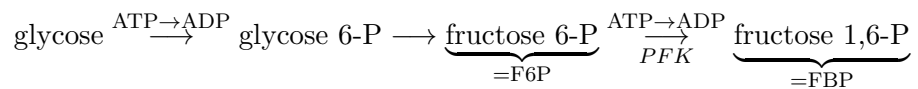
3. Biological example:

Biochemical oscillations are very common in biology, but the first ones were directly observed rather late, namely the periodic conversion of sugar to alcohol in yeast in 1964. This is a specific example for a class of oscillators called the substrate-depletion oscillator. In 1968, Selkov suggested a simple 2d mathematical model for it.

Because it is so central to evolution, sugar metabolism is extremely efficient:



The produced energy is stored in up to 36 ATP molecules. The ability to oscillate comes from the fact that ADP/ATP enters the details of this pathway in several ways:

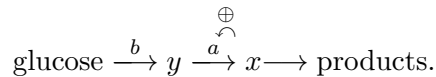


Therefore the first steps of the glycolysis pathway use up ATP rather than producing it. On the other hand, the enzyme PFK is activated by ADP, thus switching on the ATP-generating pathway on demand. We call this *autocatalysis* or a *positive feedback loop*. Overall, more ATP is produced than used up by this pathway.

In order to model these conflicting trends that eventually lead to oscillations, we introduce the following grouping:

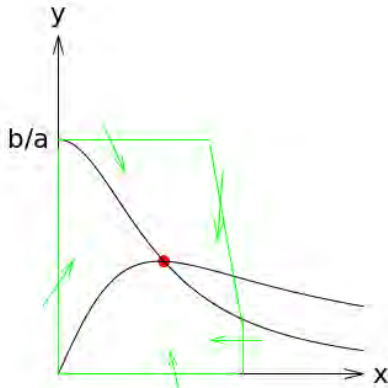
$$y = \begin{cases} \text{ATP} \\ \text{F6P} \end{cases} \quad \text{and} \quad x = \begin{cases} \text{ADP} \\ \text{FBP} \end{cases}$$

Introducing the reaction rates a , b , we get:



x is produced with a constant rate a from y and it reacts to products with a normalized rate. The production rate of x increases in proportion to its amount. We analyze the following equations:

$$\begin{aligned} \dot{x} &= -x + ay + x^2y \\ \dot{y} &= b - ay - x^2y. \end{aligned}$$



The nullclines are $y = \frac{x}{a+x^2}$ and $y = \frac{b}{a+x^2}$. So, there is a fixed point $(x^*, y^*) = (b, \frac{b}{a+b^2})$.

In order to show that a trapping region exists, we consider the region bounded by the green lines. We know for the left part $x = 0$ and $0 \leq y \leq \frac{b}{a}$. So we get $0 \leq \dot{x} \leq b$ and $0 \leq \dot{y} \leq b$. The flow goes inside. For the right part we calculate $\dot{x} - (-\dot{y}) = \dot{x} + \dot{y} = b - x < 0$ since $x > b$. This yields $-\dot{y} > \dot{x}$. Therefore, the flow is more negative than -1 and goes inside.

We have thus found a trapping region. The Poincaré-Bendixson theorem demands that no fixed points exist. Hence, we make a hole around the fixed point and show that no trajectory goes into the hole. This is equivalent to a repulsive (unstable) fixed point. The Jacobian is

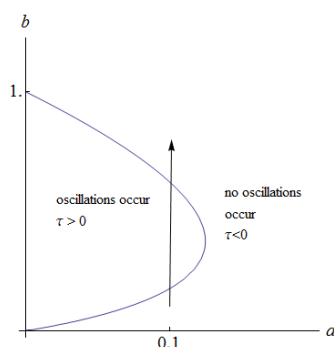
$$A = \begin{pmatrix} -1 + 2xy & a + x^2 \\ -2xy & -(a + x^2) \end{pmatrix}.$$

We need a positive trace τ and determinant Δ of the matrix A .

$$\Delta = a + b^2 > 0$$

$$\tau = \frac{b^4 + (2a - 1)b^2 + (a + a^2)}{a + b^2} \stackrel{!}{=} 0$$

Thus, the boundary between stable and unstable fixed points $\tau = 0$ is given by $b^2 = \frac{1}{2}(1 - 2a) \pm \sqrt{1 - 8a}$. This can be represented via a state-diagram.



The arrow indicates an increasing b . If a is small enough, the system performs oscillations in a certain interval of b . We call this a re-entrance process.

Lienard systems / van der Pol oscillator

The following structure often occurs in mechanics and electronics:

$$\underbrace{\ddot{x}}_{\text{inertia}} + \underbrace{f(x) \cdot \dot{x}}_{\text{damping}} + \underbrace{g(x)}_{\text{restoring force}} = 0.$$

It is called *Lienard-system*. Note, that this is the equation of the harmonic oscillator for $f = 0$ and $g = x$.

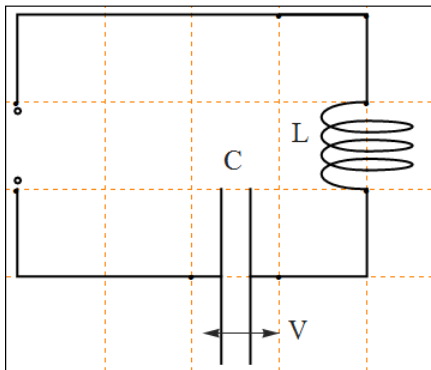
We consider the most famous example of Lienard systems, the *van der Pol oscillator*:

$$f = \mu(x^2 - 1)$$

$$g = x.$$

For $x \ll 1$ we have negative damping. The system can be driven by putting energy into the system. For large x , the damping is positive. Energy is dissipated.

Example: Tetrode circuit (electronics)



The system is described as follows:

$$\begin{aligned}
 L\dot{I} + V + F(I) &= 0 \\
 \Rightarrow L\ddot{I} + \dot{V} + F'(I)\dot{I} &= 0 \\
 \Rightarrow LC \cdot \ddot{I} + I + CF'(I) \cdot \dot{I} &= 0.
 \end{aligned}$$

This is a van der Pol oscillator with $f(I) = CF'(I)$ and $g = 1$.

Lienard systems are very widespread: e.g.

1. neural activity, action potential
2. biological oscillators (ear, circadian rhythms)
3. stick-slip oscillations in sliding friction

Lienard theorem:

A Lienard system has a stable limit cycle around the origin at the phase plane if

1. $g(-x) = -g(x)$, $g(x) > 0$ for $x > 0$
2. $f(-x) = f(x)$, $F(x) = \int_0^x f(x')dx'$ has to have a zero at $a > 0$
and $F(x) < 0$ for $0 < x < a$, $F(x) > 0$ for $x > a$, $F(\infty) = \infty$.

Obviously, the first condition is fulfilled for the van der Pol oscillator. Consider the second condition:

$$F(x) = \mu \left(\frac{x^3}{3} - x \right) = \frac{\mu x}{3} (x^2 - 3) \Rightarrow a = \sqrt{3}.$$

As for the harmonic oscillator the deflection behaves sine-shaped, the deflection of the van der Pol oscillator follows a sawtooth. The phase portrait shows a deformed circle.

Now, we analyze the van der Pol oscillator in two limits: $\mu \gg 1$ and $\mu \ll 1$.

1. $\mu \gg 1$: Lienard phase plane analysis

The dynamic equation is

$$\begin{aligned} -x &= \ddot{x} + \mu \dot{x}(x^2 - 1) = \frac{d}{dt}(\dot{x} + \mu F(x)) =: \frac{d}{dt}w(x). \\ \Rightarrow \dot{x} &= w - \mu F(x) \end{aligned}$$

In the last step, we are using $\frac{dF(x)}{dt} = f(x) \cdot \dot{x}$. Define

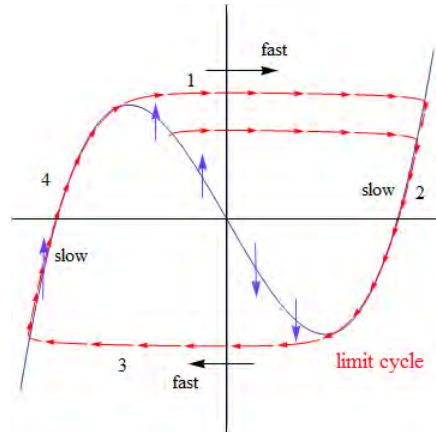
$$y := \frac{w}{\mu} \Rightarrow \boxed{\dot{y} = -\frac{x}{\mu}, \quad \dot{x} = \mu(y - F(x))}.$$

Hence, the nullclines are $x = 0$ and $y = F(x)$.

We assume the initial condition $y - F(x) \sim \mathcal{O}(1)$. Then, the velocity is very fast in x -direction but very slow in y -direction:

$$\begin{aligned} \dot{x} &\sim \mathcal{O}(\mu) \\ \dot{y} &\sim \mathcal{O}(1/\mu) \end{aligned}$$

Thus the first part shows a fast movement to the right which stops at the \dot{x} -nullcline.



In the second part, $y - F(x) \sim \mathcal{O}(1/\mu^2)$ can be arbitrarily small. This leads to $\dot{x} \sim \mathcal{O}(1/\mu)$ and $\dot{y} \sim \mathcal{O}(1/\mu)$. Thus, we have a slow movement along the nullcline. Both velocities are now negative, so we slide along the nullcline on the lower side. The third and fourth part are like the first and second, respectively, only with changed signs in the velocities.

What is the oscillation period T ? We neglect the fast paths. Hence, we have to calculate

$$T = 2 \int_{t_1}^{t_2} dt.$$

where t_1 and t_2 are the time points delimiting the fast path at the right. For t_2 we know that it corresponds to the right extremum, which is at $x_2 = 1$. For t_1 , we know that it must have the same y -value as the left extremum at $x = -1$, which is $2/3$. Therefore we have $x_1 = 2$.

We now switch from time t to position x :

$$\frac{dy}{dt} = F'(x) \frac{dx}{dt} = (x^2 - 1) \frac{dx}{dt} = -\frac{x}{\mu}$$

and from this

$$dt = dx \frac{-\mu(x^2 - 1)}{x}.$$

Therefore, the oscillation period is $T \sim \mathbb{O}(\mu)$:

$$\begin{aligned} \Rightarrow T &= 2 \int_{x_1=2}^{x_2=1} dx \frac{-\mu(x^2 - 1)}{x} = 2\mu \left[\frac{x^2}{2} - \ln(x) \right]_1^2 = \mu(3 - 2 \ln(2)) \\ \Rightarrow T &\sim \mathbb{O}(\mu). \end{aligned}$$

2. $\mu \ll 1$:

This case is a small perturbation to the harmonic oscillator

$$\ddot{x} + x + \epsilon \cdot h(x, \dot{x}) = 0.$$

The systems dynamics depend on $h(x, \dot{x})$.

- (a) For $h = (x^2 - 1)\dot{x}$, the system is a van der Pol oscillator.
- (b) For $h = 2\dot{x}$, we have a weakly damped harmonic oscillator. The system is linear.
- (c) For $h = x^3$, the system corresponds to an unharmonic spring with a spring constant $k = 1 + \epsilon x^2$ that increases by extending the spring. This is called *strain stiffening*. The system is a *Duffing oscillator*.

We first consider the second case $h = 2\dot{x}$, because this linear case can be solved exactly. This can be done by rewriting the equation of motion in two dimensions with x and v . The corresponding matrix

$A = \begin{pmatrix} 0 & 1 \\ -1 & -2\epsilon \end{pmatrix}$ has the following eigenvalues and eigenvectors:

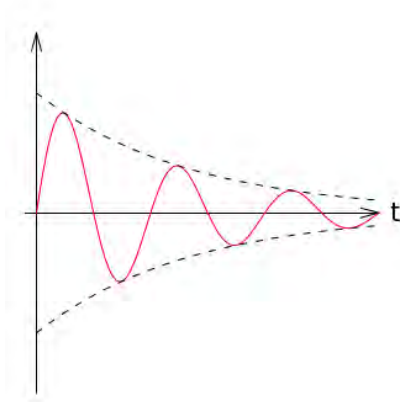
$$\lambda_{1,2} = -\epsilon \pm ic, \quad \vec{v}_{1,2} = (-\epsilon \mp ic, 1) \quad (7.0.1)$$

where $c = (1 - \epsilon^2)^{1/2}$. Thus the general solution is

$$\vec{x}(t) = (a_1 \vec{v}_1 \exp(\lambda_1 t) + a_2 \vec{v}_2 \exp(\lambda_2 t))$$

For the initial condition $\vec{x}(0) = (0, 1)$ we find $a_{1,2} = 1/2 \pm (\epsilon i)/(2c)$. Putting all this together, we get the analytical solution

$$x(t) = \frac{1}{c} \exp(-\epsilon t) \sin(ct).$$



For the initial conditions

$$x(0) = 0, \quad \dot{x}(0) = 1,$$

the exact solution reads

$$x(t) = (1 - \epsilon^2)^{-1/2} \cdot \exp(-\epsilon t) \cdot \sin((1 - \epsilon^2)^{1/2} \cdot t).$$

Thus we have a damped oscillation.

If we expand for $\epsilon \ll 1$, we find

$$x(t) = (1 - \epsilon t) \sin(t) + \mathcal{O}(\epsilon^2).$$

But, this is only valid for $t < \frac{1}{\epsilon}$ and blows up for large times. Thus, the small epsilon limit appears to be problematic.

We now try to solve the problem using regular perturbation theory. Plugging the ansatz

$$x(t) = x_0(t) + \epsilon x_1(t) + \dots$$

in the dynamic equation yields

$$\frac{d^2}{dt^2}(x_0 + \epsilon x_1 + \dots) + 2\epsilon \frac{d}{dt}(x_0 + \epsilon x_1 + \dots) + (x_0 + \epsilon x_1 + \dots) = 0.$$

Compare the parameters for different orders of ϵ .

$$\begin{aligned} \mathcal{O}(1) : \quad & \ddot{x}_0 + x_0 = 0 \\ & \Rightarrow x_0 = \sin(t) \\ \mathcal{O}(\epsilon) : \quad & \ddot{x}_1 + 2\dot{x}_0 + x_1 = 0 \\ & \Rightarrow \ddot{x}_1 + x_1 = -2\cos(t) \\ & \Rightarrow x_1(t) = -t \cdot \sin(t) \end{aligned}$$

Now, we see

$$x = x_0 + \epsilon x_1 + \mathcal{O}(\epsilon^2) \approx (1 - \epsilon t) \sin(t).$$

Again, we end up with a term that is linear in t .

The solution to this problem comes from singular perturbation theory. We separate time scale into a fast time $\tau = t$ and a slow time $T = \epsilon t$. This procedure is called *two timing* and is motivated by the fact that the exact solution has a fast time scale for the oscillations

and a slow one for the damping. Similar approaches are in general helpful for multiscale problems, such as e.g. the boundary layer in hydrodynamics.

We use the new ansatz:

$$x(t) = x_0(\tau, T) + \epsilon x_1(\tau, T) + \mathbb{O}(\epsilon^2)$$

and therefore calculate the derivatives

$$\begin{aligned} \dot{x} &= \partial_\tau x \partial_t \tau + \partial_T x \partial_t T \\ &= \partial_\tau x + \partial_T x \cdot \epsilon \\ &= \partial_\tau x_0 + \epsilon(\partial_\tau x_1 + \partial_T x_0) + \mathbb{O}(\epsilon^2) \\ \ddot{x} &= \partial_{\tau\tau} x_0 + \epsilon(\partial_{\tau\tau} x_1 + 2\partial_{T\tau} x_0) + \mathbb{O}(\epsilon^2) \end{aligned}$$

and plug them into the dynamic equation

$$\Rightarrow 0 = \partial_{\tau\tau} x_0 + \epsilon(\partial_{\tau\tau} x_1 + 2\partial_{T\tau} x_0) + 2\epsilon\partial_\tau x_0 + (x_0 + \epsilon x_1) + \mathbb{O}(\epsilon^2).$$

$$\mathbb{O}(1) : \quad \partial_{\tau\tau} x_0 + x_0 = 0$$

$$\mathbb{O}(\epsilon) : \quad \partial_{\tau\tau} x_1 + x_1 = -2(\partial_{T\tau} x_0 + \partial_\tau x_0)$$

$$\mathbb{O}(1) : \quad \Rightarrow x_0 = A(T) \sin(\tau) + B(T) \cos(\tau)$$

$$\mathbb{O}(\epsilon) : \quad \Rightarrow \partial_{\tau\tau} x_1 + x_1 = -2 \cdot (A'(T) + A(T)) \cos(\tau) + 2 \cdot (B'(T) + B(T)) \sin(\tau)$$

In order to end up with a well-behaved solution, demand the prefactors $(A' + A)$ and $(B' + B)$ to be zero.

$$\Rightarrow \quad A = A_0 \cdot \exp(-T), \quad B = B_0 \cdot \exp(-T)$$

For the initial conditions $x(0) = 0$, $\dot{x}(0) = 1 \Rightarrow B_0 = 0$, $A_0 = 1$, the general solution is sine-shaped with an envelope decaying in time

$$\Rightarrow \quad x_0 = \exp(-T) \cdot \sin(\tau) = \exp(-\epsilon t) \cdot \sin(t).$$

This is identical to the exact solution in order $\mathbb{O}(\epsilon^2)$. To do better, we had to introduce a super-slow time scale of order $\mathbb{O}(\epsilon^2)$, but at least the blow-up is avoided and we get the correct damping.

Application to van der Pol oscillator

The dynamic equation

$$\ddot{x} + \epsilon(x^2 - 1)\dot{x} + x = 0$$

holds

$$[\partial_{\tau\tau} x_0 + \epsilon(\partial_{\tau\tau} x_1 + 2\partial_{T\tau} x_0)] + \epsilon(x_0^2 - 1)\partial_\tau x_0 + (x_0 + \epsilon x_1) = 0.$$

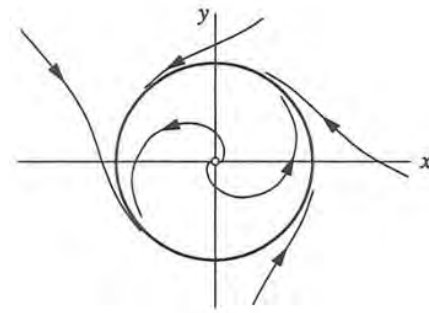
$$\mathbb{O}(1) : \partial_{\tau\tau} x_0 + x_0 = 0$$

$$\mathbb{O}(\epsilon) : \partial_{\tau\tau} x_1 + x_1 = -2\partial_{T\tau} x_0 - (x_0^2 - 1)\partial_\tau x_0$$

In polar coordinates:

$$\begin{aligned} x_0 &= r(T) \cdot \cos(\tau + \Phi(T)) \\ \Rightarrow \partial_{\tau\tau} x_1 + x_1 &= 2[r' \sin(\tau + \Phi) + r\Phi' \cos(\tau + \Phi)] + r \sin(\tau + \Phi)[r^2 \cos^2(\tau + \Phi) - 1] \\ &\quad - [2r' - r + \frac{1}{4}r^3] \sin(\tau + \Phi) + 2r\Phi' \cos(\tau + \Phi) + \frac{1}{4}r^3 \sin(3(\tau + \Phi)). \end{aligned}$$

In the last step, we used the relation $\sin(\theta) \cdot \cos^2(\theta) = \frac{1}{4}[\sin(\theta) + \sin(3\theta)]$. In order to avoid a resonance catastrophe, demand the prefactors $[2r' - r + \frac{1}{4}r^3]$ and $2r\Phi'$ to be zero.



$$\Rightarrow \boxed{r' = \frac{1}{8}r(4 - r^2)} \quad \text{and} \quad \boxed{\Phi' = 0}$$

The result is a logistic growth in r .

There is a fixed point for $r^* = 2$ and $\Phi = \text{const} = \Phi_0$.

Note, that we get a limit cycle irrespective of the value of ϵ . Therefore, ϵ is a *singular perturbation*.

Averaging method:

We now discuss a more general method to solve these kinds of problems, because obvious the procedure is always similar. Consider $\ddot{x} + x + \epsilon h(x, \dot{x}) = 0$, which represents a large class of non-linear oscillators.

$$\partial_{\tau\tau} x_0 + x_0 = 0$$

$$\partial_{\tau\tau} x_1 + x_1 = -2\partial_{T\tau} x_0 - h$$

$$\Rightarrow x_0 = r(T) \cos(\tau + \Phi(T))$$

$$\partial_{\tau\tau} x_1 + x_1 = 2[r' \sin(\tau + \Phi) + r\Phi' \cos(\tau + \Phi)] - h$$

Since we have $h(x, \dot{x}) = h(\sin(\tau + \Phi), \cos(\tau + \Phi))$, a 2π -periodic function in $\theta = \tau + \Phi$, we can use the Fourier expansion $h(\theta)$:

$$h(\theta) = \sum_{k=0}^{\infty} a_k \cos(k\theta) + \sum_{k=1}^{\infty} b_k \sin(k\theta).$$

Up to $\mathcal{O}(\epsilon)$, the only resonant terms for x_1 are $(2r' - b_1) \sin(\theta)$ and $(2r\Phi' - a_1) \cos(\theta)$. From this, we get the conditions

$$\Rightarrow r' = \frac{b_1}{2}, \quad r\Phi' = \frac{a_1}{2}$$

to avoid the resonance catastrophe. We write the Fourier coefficients in terms of averages of θ :

$$\begin{aligned} a_1 &= \frac{1}{\pi} \int_0^{2\pi} d\theta h(\theta) \cos(\theta) \\ &= 2 \langle h \cos(\theta) \rangle_\theta \\ b_1 &= 2 \langle h \sin(\theta) \rangle_\theta \end{aligned}$$

$$\Rightarrow \left. \begin{aligned} r' &= \langle h \sin(\theta) \rangle_\theta \\ r\Phi' &= \langle h \cos(\theta) \rangle_\theta \end{aligned} \right\} \text{dynamical equations for } (r, \Phi)$$

Example: van der Pol oscillator

Consider $h = (x^2 - 1)\dot{x} = (r^2 \cos^2(\theta) - 1)(-r \sin(\theta))$.

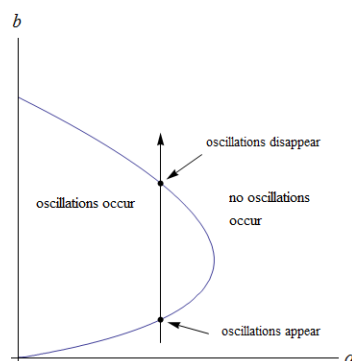
$$\begin{aligned} r' &= \langle h \sin(\theta) \rangle_\theta \\ &= -r^3 \langle \cos^2(\theta) \sin^2(\theta) \rangle_\theta + r \langle \sin^2(\theta) \rangle \\ &= \frac{1}{2}r - \frac{1}{8}r^3 \\ &= \frac{1}{8}r(4 - r^2) \quad \Rightarrow \boxed{r^* = 2} \\ r\Phi' &= \langle h \cos(\theta) \rangle_\theta \\ &= -r \underbrace{\langle \sin(\theta) \cos(\theta) \rangle_\theta}_{=0} - r^3 \underbrace{\langle \cos^3(\theta) \sin(\theta) \rangle_\theta}_{=0} \\ &= 0 \quad \Rightarrow \boxed{\Phi = \text{const}} \end{aligned}$$

This is the same result as before, as it should be.

Chapter 8

Bifurcations in 2d

Like in 1d, in 2d existence and stability of fixed points depend on the parameters of the system. In contrast to 1d, however, now also oscillations can be switched on and off. As an example, look at the substrate-depletion-oscillator.



There are three types of bifurcations in 2d:

1. 1d-like bifurcations (4 types)
2. Hopf bifurcation (local switch on/off of oscillations)
3. global bifurcations of cycles (3 types)

In the following, we have a closer look at them.

1. 1d-like bifurcations

All four types of 1d bifurcations exist in 2d (cf. *center manifold theorem*).

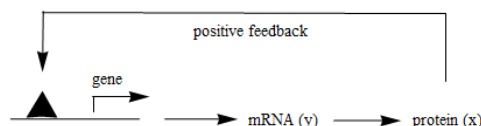
Example: Griffith model for genetic switch

Consider a gene that codes for a certain protein. The activity of the gene shall be induced by the protein and its copies which are translated from the messenger RNA. The system is described as

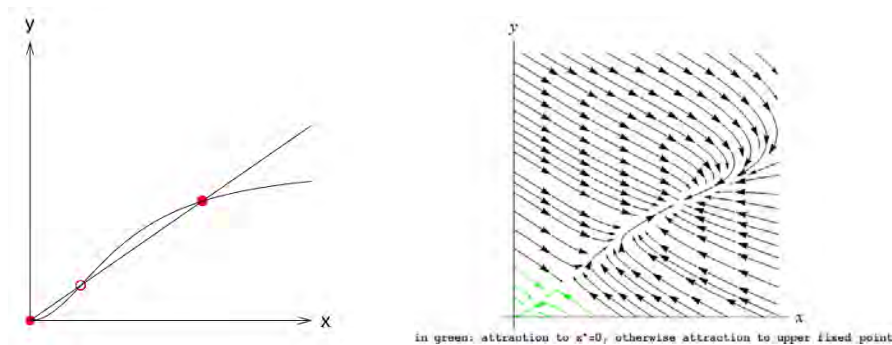
$$\begin{aligned} \dot{x} &= y - ax \\ \dot{y} &= \frac{x^2}{1+x^2} - by, \end{aligned}$$

where, x and y are the concentrations of the protein and the mRNA, respectively.

The following figure shows a protein acting as transcription factor.



The nullclines are $y = a \cdot x$ and $y = \frac{x^2}{b(1+x^2)}$. We see that the system depends on the parameters a , b . For increasing a , the two upper fixed points approach each other until they fall together when the nullclines intersect tangentially. For even larger a , only the fixed point in the origin remains.



The two upper fixed points are given by

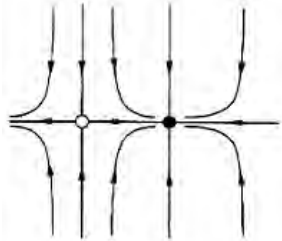
$$\begin{aligned} x^* &= ab(1 + x^{*2}) \\ \Rightarrow x^* &= \frac{1 \pm \sqrt{1 - 4a^2b^2}}{2ab}. \end{aligned}$$

For $2ab = 1$, the fixed points collide. The critical values are

$$a_c = \frac{1}{2b} \quad x_c^* = 1.$$

If $a < a_c$, the system is bistable and acts like a genetic switch: depending on the initial conditions, the gene is on or off.

We note that in this case, the 2d analysis gives essentially the same results like a 1d analysis along the x -nullcline. In fact, this is an example of a saddle-node bifurcation.



The prototype of a saddle-node bifurcation in 2d is

$$\begin{aligned}\dot{x} &= \mu - x^2 \\ \dot{y} &= -y.\end{aligned}$$

The phase portrait varies with μ .

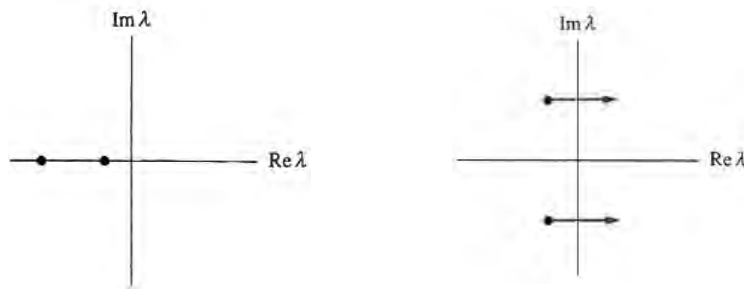
One fixed point is a saddle, $x^* = (-\sqrt{\mu}, 0)$, the other one a stable node, $x^* = (+\sqrt{\mu}, 0)$. The behavior of the saddle depends on the eigenvalues λ of the Jacobian $A = \begin{pmatrix} -2x^* & 0 \\ 0 & -1 \end{pmatrix}$ with $x^* = (-\sqrt{\mu}, 0)$. The bifurcation is given for $\lambda = 0$. This is called a *zero eigenvalue-bifurcation*. It exists for all bifurcations from type 1).

Recall that the eigenvalues can be calculated using

$$\lambda_{1/2} = \frac{\tau \pm \sqrt{\tau^2 - 4\Delta}}{2}.$$

Either both eigenvalues are real (shown on the left), which corresponds to $(\tau^2 - 4\Delta) > 0$, or they are complex (shown on the right), $(\tau^2 - 4\Delta) < 0 \Rightarrow \lambda_{1/2} = \frac{\tau}{2} \pm i\omega$.

The saddle-node bifurcation is of the first type. We now turn to the second type.



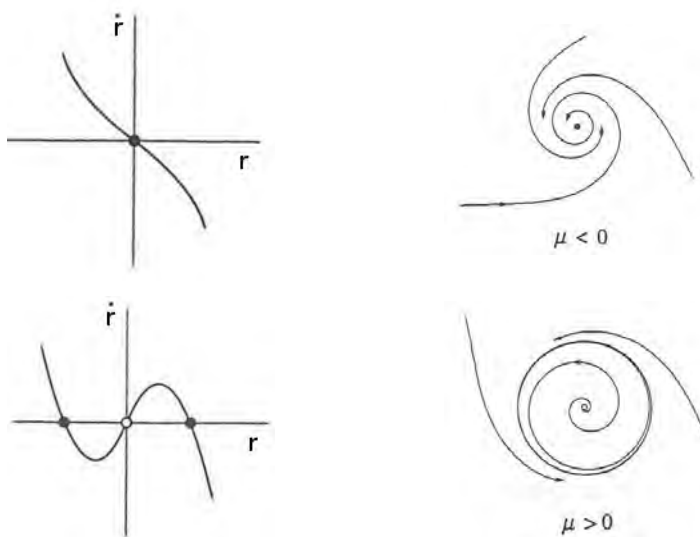
If the complex eigenvalues $\lambda_{1/2} = \frac{\tau}{2} \pm i\omega$ cross the y -axis from left to right, oscillations are switched on. This is called *Hopf bifurcation*.

2. Hopf bifurcation

(a) Supercritical Hopf bifurcation

$$\begin{aligned}\dot{r} &= \mu r - r^3 \\ \dot{\theta} &= \omega + br^2\end{aligned}$$

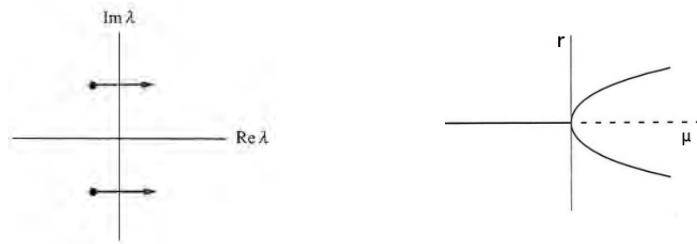
The systems dynamics strongly depends on μ .



In order to analyze the behavior of the eigenvalues during the bifurcation, rewrite the system in Cartesian coordinates:

$$\begin{aligned}x &= r \cos(\theta) \\ y &= r \sin(\theta) \\ \dot{x} &= \dot{r} \cos(\theta) - r \sin(\theta) \dot{\theta} \\ &= \mu x - \omega y + \mathcal{O}(xr^2, yr^2) \\ \dot{y} &= \omega x + \mu y \\ \Rightarrow A &= \begin{pmatrix} \mu & -\omega \\ \omega & \mu \end{pmatrix} \\ \Rightarrow \lambda_{1/2} &= \mu \pm i\omega\end{aligned}$$

Thus, if we increase μ , the eigenvalues cross the imaginary axis from left to right as expected.

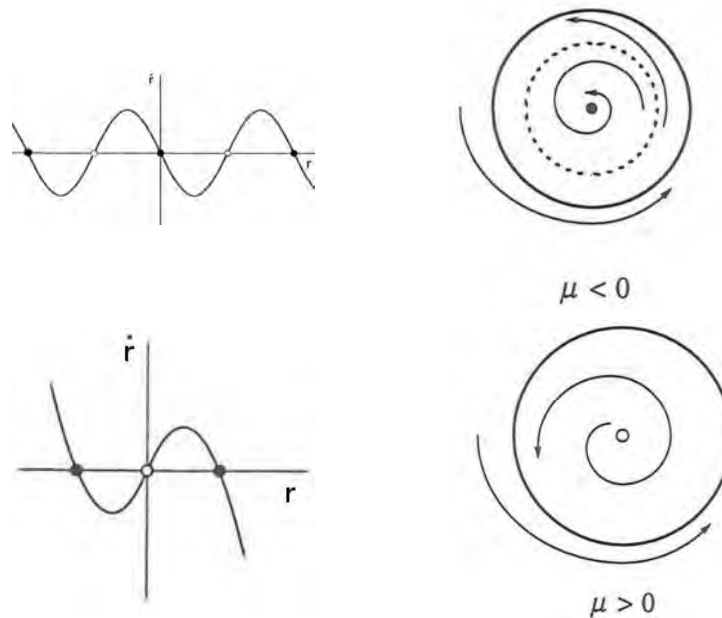


The structure is similar to the supercritical pitchfork bifurcation. But now, we have a *supercritical Hopf bifurcation*.

(b) Subcritical Hopf bifurcation

$$\begin{aligned}\dot{r} &= \mu r + r^3 - r^5 \\ \dot{\theta} &= \omega + br^2\end{aligned}$$

The term $(-r^5)$ causes certain trajectories to drive away from the origin. For $\mu < 0$, both exist a stable limit cycle and an attractive fixed point in the origin. But for increasing μ , the attractive area around the origin decreases and finally disappears for $\mu = 0$. That is when the subcritical Hopf bifurcation occurs. The origin is now unstable and there is an abrupt transition to large-amplitude oscillations.



Note that a Hopf bifurcation theorem exists, demanding rigorous conditions on $\lambda_{1/2}$ for a Hopf bifurcation to occur.

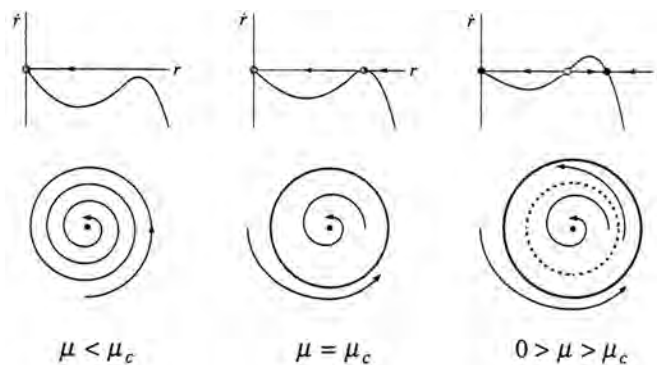
3. Global bifurcations of cycles

Apart from Hopf bifurcations, global bifurcations are another way in which limit cycles are created or destroyed. They are a combination of 1) and 2). Cycle interactions with other fixed points exist. As well, there is a global change in flow structure.

(a) Saddle-node bifurcation of circles

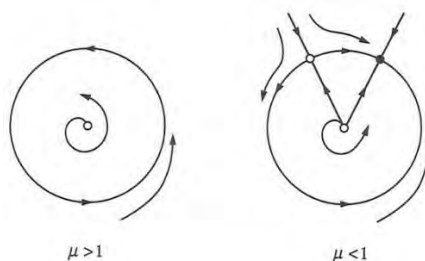
This is a prototypical example of global bifurcations.

$$\begin{aligned}\dot{r} &= \mu r + r^3 - r^5 \\ \dot{\theta} &= \omega + br^2 \\ \mu_c &= -\frac{1}{4}\end{aligned}$$



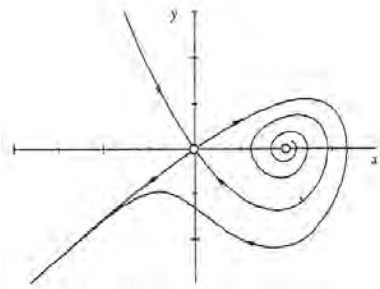
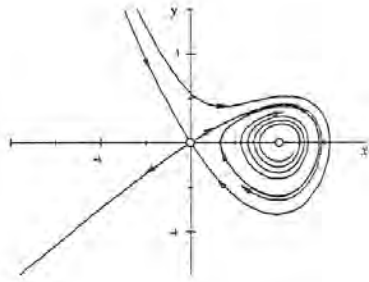
(b) Infinite period bifurcation

$$\begin{aligned}\dot{r} &= r(1 - r^2) \\ \dot{\theta} &= \mu - \sin(\theta) \\ \mu_c &= 1\end{aligned}$$



(c) Homoclinic bifurcation

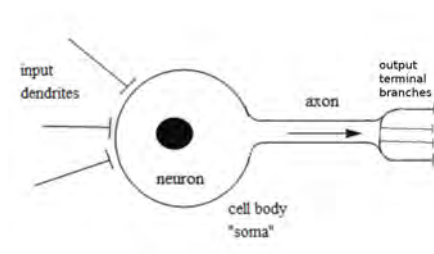
$$\begin{aligned}\dot{x} &= y \\ \dot{y} &= \mu y + x - x^2 + xy \\ \mu_c &\approx 8.6\end{aligned}$$



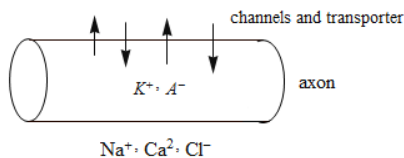
Chapter 9

Excitable systems

In this chapter, we discuss so-called "excitable systems". One example is grass, that is burned down and then regrows. Obviously, this process can be repeated over and over again. We also see that such a process can occur in the spatial domain as a wave. Our biological example is neuronal activity in the brain. Here, the wave is called an "action potential" and it travels along the axon of a neuron.



A human neuron has a diameter of $r \approx 50 \mu\text{m}$ for the cell body and an axon that is up to 1 m long. The axon transports the signals called *action potentials* or *spikes*. We think about them as traveling waves $V(x, t)$.

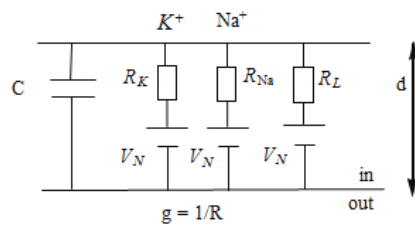


It is approximately cylindrically shaped containing mainly potassium (K^+) and organic anions (A^-) and being surrounded predominantly by sodium (Na^+), calcium (Ca^{2+}) and chlorine (Cl^-).

Typical values of the concentrations of the two dominant ions potassium and sodium are given in the following table:

	inside [mM]	outside [mM]	ΔV [mV]
K^+	155	4	-98
Na^+	12	154	67

The axon membrane is typically 5 nm thick and made of dielectric material ($\epsilon = 2$) which is an insulator. To allow ion flow, there are many channels in the surface. Channels can dynamically open and close. The resting potential is approximately $\Delta V = -60$ mV. Here is an equivalent electrical circuit:



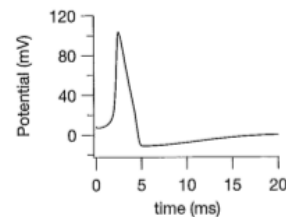
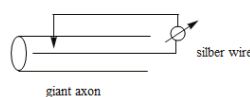
A biological membrane acts as a capacitor for which the equation $C_A = \frac{C}{A} = \frac{\epsilon_0 \epsilon}{d}$ holds. Typically, $\frac{C}{A}$ is around $\frac{\mu F}{cm^2}$. The timescale is $\tau = \frac{C_A}{g_A} = \frac{C}{g} \approx 2$ ms with the conductivity per area $g_A = 5 \frac{1}{\Omega m^2}$.

Assuming equilibrium, the concentration c is proportional to a Boltzmann distribution $c \sim \exp(-eV/k_B T)$. The ratio of the concentrations inside and outside of the axon therefore depends on the difference of the potential $\frac{c_i}{c_o} \sim \exp(-e(V_i - V_o)/k_B T)$. Solving for the difference of the potential, this yields the *Nernst potential*:

$$\Rightarrow \Delta V = \frac{k_B T}{e} \cdot \ln \left(\frac{c_i}{c_o} \right).$$

This equation has been used to calculate ΔV in the previous table ($\frac{k_B T}{e} = 25$ mV). Since $\Delta V_1 \neq \Delta V_2$, the system is not in equilibrium.

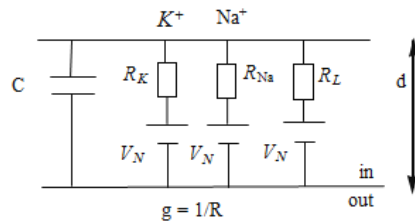
The exact form of an action potential can be measured with a *space clamp*. Taking a giant axon of a squid and threading a silver wire into the axon, the action potential $V(t) = V_i(t) - V_o(t)$ can be determined independent from spatial components.



1938	Hodgkin worked at Woods Hole (with Cole). Cole later invented the space clamp.
1949	Hodgkin performed experiments with the space clamp at Plymouth together with his student Huxley.
1952	Famous Hodgkin and Huxley papers (some together with Katz): the dynamics of so-called <i>gates</i> produce temporal changes in conductivity
1960	Richard FitzHugh and later Nagumo et al. independently analyzed a reduced HH-model with phase plane analysis, leading to the standard NLD-model for action potentials
1963	Nobel prize for Hodgkin and Huxley (together with John Eccles, who worked on motorneuron synapses)
1991	Nobel prize for Erwin Neher and Bert Sakmann for the patch clamp technique: the molecular basis of an action potential could be demonstrated directly for the first time
2003	Nobel prize for Roderick MacKinnon for his work (Science 1998) on the structure of the K^+ channel, which in particular explained why Na^+ ions cannot pass
May 2012	Andrew Huxley dies at the age of 94; after his work on the action potential, he revolutionized muscle research (the sliding filament hypothesis from 1954 and the Huxley model for contraction from 1957 could have earned him a second Nobel prize)

Table 9.1: Overview historical development.

Hodgkin-Huxley model (1952)



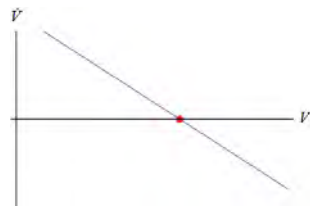
Starting with the electrical circuit, Hodgkin and Huxley invented a model for action potentials. They assumed a linear relation between voltage and current

$$I_{Na} = g_{Na}(V - V_{Na}).$$

Faraday's law states $Q = C \cdot V \Rightarrow I = C \cdot \dot{V}$.

$$\Rightarrow \dot{V} = -\frac{1}{C} \left[g_{Na}(V - V_{Na}) + g_K(V - V_K) + \underbrace{g_L(V - V_L)}_{\text{leakage current}} \right]$$

The leakage current contains all contributions except those from potassium and sodium.



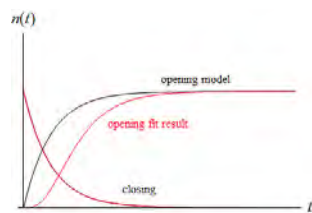
This equations describes a linear system with a stable fixed point. If a little perturbation occurs the system will relaxing back. But this behavior does not fit to the experiments.

Hence, to get an action potential we consider a conductivity that depends on voltage, $g = g(V)$. The basic idea is a two-state process for opening and closing of the gate. Such a process can be described in the following way using the opening and closing probabilities α_n and β_n , respectively.

$$\dot{n} = \alpha_n(1 - n) - \beta_n \cdot n.$$

A closed gate corresponds to $n = 0$, an open one to $n = 1$. Therefore, the time-dependent processes are

$$\begin{aligned} \text{opening: } & n(t) = 1 - \exp(-t) \\ \text{closing: } & n(t) = \exp(-t). \end{aligned}$$



A voltage clamp experiment showed a good agreement for the closing process. But the fit result of the opening process corresponds to power four. In general, higher powers and three gates are needed to fit the data.

We use a four-dimensional model (V, n, m, h) defined by the additional equation

$$\begin{aligned}\dot{n} &= \alpha_n(1 - n) - \beta_n n \\ \dot{m} &= \alpha_m(1 - m) - \beta_m m \\ \dot{h} &= \alpha_h(1 - h) - \beta_h h.\end{aligned}$$

n , m and h label the potassium and sodium activation and the sodium deactivation gates, respectively. Phenomenologically, the coupling to the conductivities is

$$\begin{aligned}g_{Na} &= 120 \cdot m^3 h \\ g_K &= 36 \cdot n^4 \\ g_L &= 0.3.\end{aligned}$$

because only in this way one can understand the sigmoidal opening curves measured experimentally. The justification for the microscopic gate dynamics (the ion channels) came only 30 years later. We can interpret the powers as

$$\begin{aligned}n^4: & \text{ potassium 4 gates open} \\ m^3: & \text{ sodium 3 gates open} \\ h: & \text{ sodium 1 gate closed}\end{aligned}$$

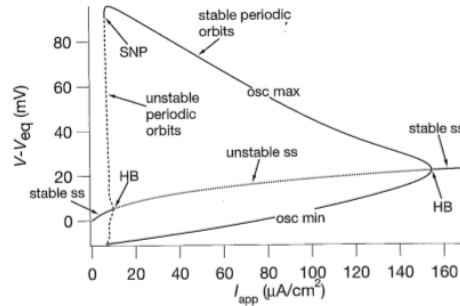
The parameters (α_i, β_i) are non-trivial functions of V . For example for n

$$\alpha_n = \frac{10 - V}{100(\exp((10 - V)/10) - 1)}, \quad \beta_n = \frac{125 \exp(-V/80)}{1000}.$$

Today, again, the six parameters can be understood from the physics of ion channels. Now, we've got a complete 4d model and we have to integrate the ODEs. We end up with the following time-dependence of the gates and the conductivities.



A more general NLD-analysis shows that the system can oscillate.

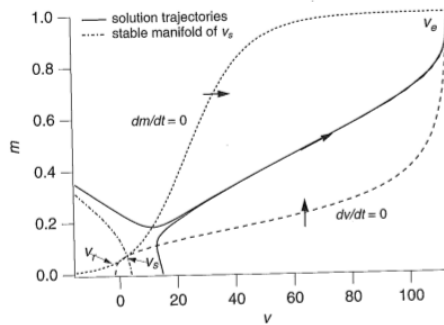


Fitzhugh-Nagumo model

For an in-depth analysis of the Hodgkin-Huxley model, Fitzhugh in the 1960s used 2D phase plane obtained as cuts through 4D phase space. He first used the two fast variables V and m and kept n and h constant. The two equations then read

$$\begin{aligned} e\dot{V} &= -\bar{g}_K n_0^4 (V - V_K) - \bar{g}_{Na} m^3 h_0 (V - V_{Na}) - \bar{g}_L (V - V_L) \\ \dot{m} &= \alpha_m^{(V)} (1 - m) - \beta_m^{(V)} \cdot m \end{aligned}$$

with the parameters \bar{g} denoting constants. The phase plane dependency of m and V is shown in the figure below.



This analysis explains the threshold between a resting and an excited state, but not the relaxation, because this comes later. Then the V -nullcline moves up and the excited state vanishes in a saddle-node bifurcation.

As a next step, Fitzhugh considered one fast variable v responsible for the excitation and a slow variable n responsible for the relaxation. He found that the v -nullcline has a cubic shape, that there is one fixed point and that the action potential is emerging as a long excursion away and back

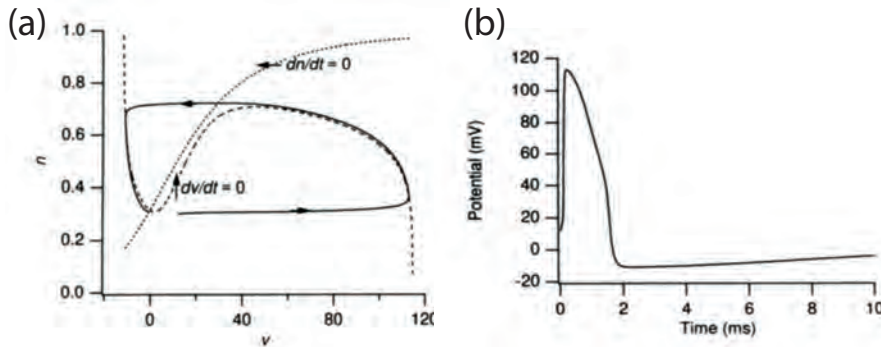


Figure 9.1: (a) Fast-slow phase plane of the Hodgkin-Huxley model. The FitzHugh-Nagumo model essentially has the same structure. (b) The resulting action potential. Taken from Keener and Sneyd.

to the fixed point guided by the cubic nullcline, compare figure 9.1. This reduction of the HH-equations then motivated him to define an even more abstract model that later became to be known as the **FitzHugh-Nagumo model** (Nagumo and coworkers built this model as an electronic circuit and published in 1964). This model assumes two variables, one slow (w) and one fast (v). The fast (excitation) variable has a cubic nullcline and the slow (recovery) variable has a linear one. There is a single intersection which is assumed to be at the origin without loss of generality. Thus the model equations are

$$\epsilon \frac{dv}{dt} = v(1-v)(v-\alpha) - w + I_{app} \quad (9.0.1)$$

$$\frac{dw}{dt} = v - \gamma w \quad (9.0.2)$$

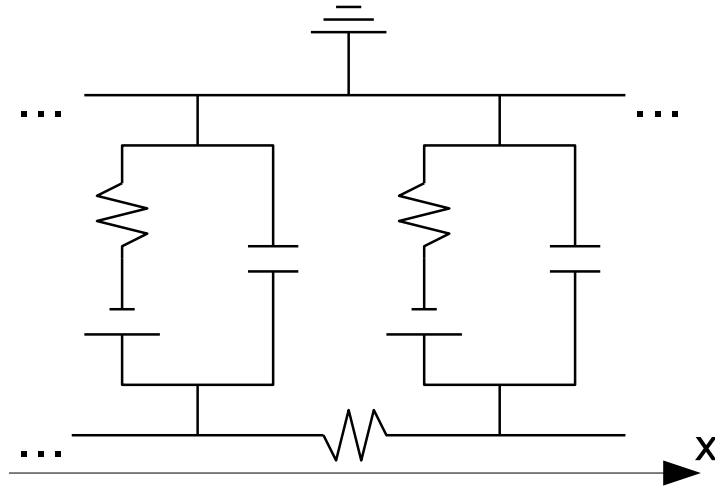
where I_{app} allows for an externally applied current, $\epsilon \ll 1$ and $0 < \alpha < 1$. Typical values are $\epsilon = 0.01$, $\alpha = 0.1$ and $\gamma = 0.5$. The phase plane analysis then show that an excitation to a small value of v leads to a large excursion (action potential) leading to the steady state $(0, 0)$. If one injects a current $I_{app} = 0.5$, the fixed point becomes unstable and a stable limit cycle emerges through a Hopf bifurction, thus the system becomes oscillatory (essential it becomes a van der Pol oscillator). Thus this simple model reproduces the main features of the HH-model.

Interestingly, the HH- and FN-models have many more interesting features if studied for a time-dependent current $I_{app}(t)$. For example, one finds that the system does not start to spike if the current is increase slowly rather than in a step-wise fashion. Thus it does not has a fixed threshold but goes super-threshold only if the current change is fast. Another interesting

observation is that an inhibitory step (negative step function) triggers a spike at the end rather than at the start of the stimulation period. Thus the direction in which the current is changed matters.

Cable equation

Up to now, we did not consider the effects of space. We now couple many HH-elements in series to describe wave propagation along the axon.



Describing the signal as traveling wave, Ohm's law holds in lateral direction

$$V(x + \Delta x) - V(x) = -I(x) \frac{\rho}{\pi r^2} dx$$

where $\rho = 0.3 \Omega m$ is the resistivity of the medium and $r = 250 \mu m$ is the radius of the squid giant axon. Looking at a node of the circuit, current conservation demands

$$I(x + \Delta x) - I(x) = -g_A(2\pi r)V(x)dx$$

Taking $\Delta x \rightarrow 0$, this yields

$$\begin{aligned} V'(x) &= -\frac{\rho}{\pi r^2} I(x) \\ I'(x) &= -g_A \cdot 2\pi r \cdot V(x) \\ \Rightarrow V''(x) &= \frac{1}{\lambda^2} V \end{aligned}$$

In the last step, the decay length $\lambda = \sqrt{\frac{r}{2\rho g_A}} = 9 \text{ mm}$ has been introduced.

Injecting a voltage V_0 at left and asking for a decaying voltage at the right, the space dependence is

$$V(x) = V_0 \cdot \exp\left(-\frac{x}{\lambda}\right).$$

Because of this, the signal would just decay if the conductivities were independent from the voltage. This has been found earlier by Lord Kelvin when investigating the decay of a signal along a passive cable like the transatlantic cable.

We next combine the longitudinal equation with the full transverse Hodgkin-Huxley current for the current conservation

$$I' = -[g_{Na}(V - V_N^{Na}) + g_K(V - V_N^K) + g_L(V - V_N^L)] - C \frac{\partial U}{\partial t}.$$

$$\Rightarrow \boxed{\lambda^2 V'' - \tau \dot{V} = \frac{g_{Na}(V - V_N^{Na}) + g_K(V - V_N^K) + g_L(V - V_N^L)}{g}}.$$

The result is a non-linear PDE, the "cable equation" with time-dependent conductivity.

Considering one type of channel (e.g. Na) and injecting a voltage V_0 at the left, a *front* propagates to the right. To get a *wave* propagation, one has to add a counteracting process (e.g. opening of K channels). Hodgkin and Huxley showed the waves in 1952. To understand this better, we consider the *bistable cable equation*

$$\dot{V} = V'' + f(V)$$

with $f(V) = -V(V - \alpha)(V - 1)$. We look for solutions of the form $V(x, t) = U(x + c \cdot t)$ which describe waves propagating from right to left with velocity c . Defining $y := x + ct$, we can convert the system into an ODE.

$$\boxed{\partial_y U \cdot c = \partial_y^2 U + f(U)}$$

Now, we do a phase plane analysis and therefore define

$$W = \partial_y U \quad \Rightarrow \quad \partial_y W = c \cdot W - f(U), \quad f(U) = -U(U - \alpha)(U - 1).$$

A traveling front solution must connect the fixed points $(U = 0, W = 0)$ and $(U = 1, W = 0)$ in the (U, W) -plane as we vary y from $-\infty$ to $+\infty$. There is a unique c^* which results in such a trajectory (finding this unique value is called *shooting*). It can be calculated analytically. For this, we guess that the connection between the two resting states is given by

$$W(U) = \frac{dU}{dy} = -BU(U - 1).$$

So, we calculate

$$\begin{aligned}
0 &= -\partial_y U \cdot c + \partial_y^2 U + f(U) \\
&= -W \cdot c + \partial_y W + f(U) \\
&= -W \cdot c + \partial_U W \partial_y U + f(U) \\
&= -cBU(U-1) + B^2(2U-1) \cdot U(U-1) - U(U-\alpha)(U-1) \\
&= cB + B^2(2U-1) - (U-\alpha)
\end{aligned}$$

Because this has to vanish for any U , we find

$$B = \frac{1}{\sqrt{2}}, \quad \boxed{c = \frac{1}{\sqrt{2}}(1 - 2\alpha)}.$$

The speed is a decreasing function of α and the direction of propagation changes at $\alpha = \frac{1}{2}$. In this case, there is no propagation. The profile of the traveling front is found by integrating the assumption

$$\begin{aligned}
W(U) &= \frac{dU}{dy} = -BU(U-1). \\
\Rightarrow U(y) &= \frac{1}{2} \left[1 + \tanh \left(\frac{1}{2\sqrt{2}} y \right) \right].
\end{aligned}$$

A propagating wave is a trajectory which comes back to the original state. This occurs in the Hodgkin-Huxley model as well as in the Fitzhugh-Nagumo model with diffusive coupling

$$\begin{aligned}
\dot{V} &= V'' + f(V, W) \\
\dot{W} &= g(V, W).
\end{aligned}$$

Until now, we studied 1d wave propagation. The cable equation can also be extended to 2d or 3d. We then obtain propagation fronts (planar or circular), but also spirals. In the context of heart and muscle biology, spirals are a sign of a pathophysiological situation.

Chapter 10

Reaction-diffusion systems

We started this lecture with the central equation

$$\frac{d\vec{x}}{dt} = \vec{f}(\vec{x})$$

which mathematically is an ODE. We now add space in the form of diffusion

$$\frac{d\vec{x}}{dt} = \vec{f}(\vec{x}) + D\Delta\vec{x}$$

where D is the diagonal matrix of the diffusion constants (a non-diagonal coupling could exist in hydrodynamic theories). Mathematically we now deal with a PDE, similar to the Schrödinger equation, the Maxwell equations or the Fokker-Planck equation. Naively, one might think that diffusion stabilizes the system, but Alan Turing showed in 1952 that there exist diffusion-driven instabilities (in a similar vein, stochastic noise can either stabilize or destabilize a system). Turing suggested that diffusion-driven instabilities might account for the spontaneous emergence of patterns in morphogenesis of animals (like the stripes of zebra or the spots of the leopard). Although it is hard to identify Turing instabilities in development, it is clear that they are very important in (bio)chemical networks. Here we introduce the main ideas and results of Turing¹.

Turing investigated under which condition a reaction-diffusion system produces a heterogeneous spatial pattern. To answer this question, he considered a two-dimensional system of the type:

$$\begin{aligned}\dot{A} &= F(A, B) + D_A\Delta A \\ \dot{B} &= G(A, B) + D_B\Delta B.\end{aligned}$$

¹For a detailed discussion, consult the book on Mathematical Biology by JD Murray, Springer, 3rd edition 2003.

A simple choice for the reaction part would be the activator-inhibitor model from Gierer and Meinhardt, where species A is autocatalytic and activates B, while B inhibits A. An even simpler choice is the activator-inhibitor model from Schnackenberg, where the autocatalytic species A is the inhibitor of B and B activates A. Both models form stripes in the Turing version and here we choose the second one because it is mathematically easier to analyse:

$$\begin{aligned} F &= k_1 - k_2 A + k_3 A^2 B \\ G &= k_4 - k_3 A^2 B. \end{aligned}$$

We first non-dimensionalize the system:

$$\begin{aligned} u &= A \left(\frac{k_3}{k_2} \right)^{1/2}, & v &= B \left(\frac{k_3}{k_2} \right)^{1/2}, \\ t &= \frac{D_A t}{L^2}, & x &= \frac{x}{L}, & d &= \frac{D_B}{D_A}, \\ a &= \frac{k_1}{k_2} \left(\frac{k_3}{k_2} \right)^{1/2}, & b &= \frac{k_4}{k_2} \left(\frac{k_3}{k_2} \right)^{1/2}, \\ \gamma &= \frac{L^2 k_2}{D_A} \end{aligned}$$

Note that the variables u and v are positive since they are concentrations of reactants. By introducing the variables above, the system is described as follows

$$\begin{aligned} \dot{u} &= \gamma \underbrace{(a - u + u^2 v)}_{=:f(u,v)} + \Delta u \\ \dot{v} &= \gamma \underbrace{(b - u^2 v)}_{=:f(u,v)} + d \Delta v \end{aligned}$$

with the ratio of the diffusion d and the relative strength of the reaction versus the diffusion terms γ which scales as $\gamma \sim L^2$.

We first consider the case without diffusion $D = 0$ and ask for a homogeneous state which is stable; we then ask under which conditions diffusion leads to an instability, the *Turing instability*.

Stabilizing diffusion. 1D reaction-diffusion system

For single reactant $u(x, t)$ there is no Turing instability:

$$u_t = D u_{xx} + f(u), \quad x \in [0, l] + \text{BC}$$

An "uniform" (x - independent) ODE

$$\dot{u} = f(u)$$

has either: stable $m = f'(u^*) < 0$, or unstable $m > 0$ equilibrium at stationary point $u^* : f(u^*) = 0$.

The diffusion will maintain a stable one, and it can stabilize the unstable one.

To check it we take the linearized problem about u^* , for $v(x, t) = u(x, t) - u^*$:

$$\begin{cases} v_t = Dv_{xx} + mv, & x \in [0, l] \\ m = f'(u^*) \end{cases}$$

We use the Neumann BC (no flux):

$$\partial_x v \Big|_{0,l} = 0$$

and eigenfunction expansion.

Separation of variables: look for the solution in the form:

$$v(x, t) = \varphi(t) \cdot \psi(x)$$

Leading to:

$$\begin{aligned} \varphi' \cdot \psi &= \varphi \cdot (D \cdot \psi'' + m \cdot \psi) \\ \Rightarrow \frac{\varphi'}{\varphi} &= \frac{D\psi'' + m\psi}{\psi} =: \mu \end{aligned}$$

Hence, the solution stability depends on the sign of μ :

$$\varphi(t) \approx \exp(\mu t)$$

The second equation:

$$D\psi'' + (m - \mu)\psi = 0, \quad \psi(0, l) = 0$$

or

$$\psi'' + \lambda^2 \psi = 0, \quad \lambda^2 = \frac{m - \mu}{D}$$

The eigenfunctions are:

$$\psi_k(x) = \cos \lambda_k x = \cos \frac{\pi k x}{l}, \quad k = 0, 1, \dots$$

Using the expression for λ we get:

$$\mu = m - D \left(\frac{\pi k x}{l} \right)^2$$

So:

- stable case ($m < 0$) remains stable,
- For unstable case the system get bifurcation values at $D \left(\frac{\pi k x}{l} \right)^2 = m$. The diffusion stabilize the unstable "uniform" equilibrium.

2d reaction-diffusion system

We now turn to two dimensions, where the Turing instability occurs. So let's start with a linear stability analysis of the reaction part using $\vec{W} = \begin{pmatrix} u - u^* \\ v - v^* \end{pmatrix}$. We denote the steady state with $\vec{W}^* = \begin{pmatrix} u^* \\ v^* \end{pmatrix}$ and a partial derivative with $f_u = \frac{\partial f}{\partial u}$ etc. This yields

$$\dot{\vec{W}} = \gamma A \vec{W}$$

with the matrix

$$A = \begin{pmatrix} f_u & f_v \\ g_u & g_v \end{pmatrix} \Big|_{\vec{W}^*}.$$

Linear stability is guaranteed if the real part of the eigenvalues λ is smaller than zero, $\text{Re } \lambda < 0$. Thus, the trace of A is smaller than zero

$$\text{tr } A = f_u + g_v < 0 \quad (10.0.1)$$

and the determinant larger than zero

$$\det A = f_u g_v - f_v g_u > 0. \quad (10.0.2)$$

The u - and v - nullcline is given by setting $f = 0$ and $g = 0$, respectively.

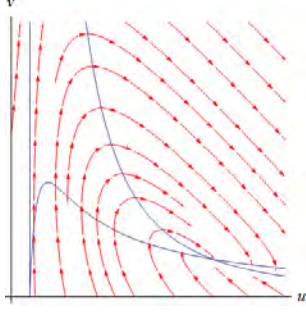
$$\begin{aligned} u\text{-nullcline: } v &= \frac{u - a}{u^2} \\ v\text{-nullcline: } v &= \frac{b}{u^2} \end{aligned}$$

For the steady state $\vec{W}^* = \begin{pmatrix} u^* \\ v^* \end{pmatrix}$, we demand u^* and v^* to be positive for physical reasons.

$$\Rightarrow (u^*, v^*) = \left(a + b, \frac{b}{(a + b)^2} \right)$$

Thus, it is $a + b > 0$ and $b > 0$.

$$\Rightarrow A = \begin{pmatrix} -1 + 2uv & u^2 \\ -2uv & -u^2 \end{pmatrix} \Big|_{\vec{W}^*} = \begin{pmatrix} \frac{b-a}{b+a} & (a+b)^2 \\ \frac{-2ab}{a+b} & -(a+b)^2 \end{pmatrix} \Rightarrow \det A = (a+b)^2 > 0$$



We get a stable spiral for $b = 2$ and $a = 0.2$.

We now turn to the full reaction-diffusion system and linearize it about the steady state

$$\dot{\vec{W}} = \gamma A \vec{W} + D \Delta \vec{W}$$

with $D = \begin{pmatrix} 1 & 0 \\ 0 & d \end{pmatrix}$.

In order to obtain an ODE from this PDE, we use the solutions of the Helmholtz wave equation

$$\Delta \vec{W} + k^2 \vec{W} = 0$$

with no-flux boundary of size p in 1d, we have

$$\vec{W}_k(x) \sim \cos(k \cdot x)$$

with wavenumber $k = \frac{n\pi}{p}$ and wavelength $\lambda = \frac{2\pi}{k} = \frac{2p}{n}$ (n integer).

$$\Rightarrow \vec{W}(\vec{r}, t) = \sum_k c_k \exp(\lambda t) \vec{W}_k(\vec{r})$$

$$\Rightarrow \lambda \vec{W}_k = \gamma A \vec{W}_k - D k^2 \vec{W}_k$$

We now have to solve this eigenvalue problem. A Turing instability occurs if $\text{Re } \lambda(k) > 0$. Our side constraint is that the eigenvalue problem for $D = 0$ (only reactions) is assumed to be stable, that is $\text{Re } \lambda(k=0) < 0$.

$$\Rightarrow 0 = \lambda^2 + \lambda[k^2(1+d) - \gamma \text{tr } A] + [dk^4 - \gamma(df_u + g_v)k^2 + \gamma^2 \det A].$$

We first note that the coefficient of λ is always positive because $k^2(1+d) > 0$ and $\text{tr } A < 0$ (for reasons of the stability of the reaction system). In order

to get an instability, $\text{Re } \lambda > 0$, the constant part has to be negative. Since the first and last terms are positive, this implies

$$df_u + g_v > 0 \quad \Rightarrow \quad d \neq 1. \quad (10.0.3)$$

This is the main result by Turing: An instability can occur if one component diffuses faster than the other. (10.0.3) is only a necessary, but not a sufficient condition. We require that the constant term as a function of k^2 has a negative minimum.

$$\frac{(df_u + g_v)^2}{4d} > \det A = f_u g_v - f_v g_u \quad (10.0.4)$$

The critical wavenumber can be calculated to be

$$k_c = \gamma \left(\frac{\det A}{d_c} \right)^{1/2}$$

with the critical diffusion constant from

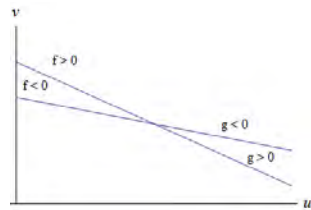
$$d_c^2 f_u^2 + 2(2f_v g_u - f_u g_v) d_c + g_v^2 = 0.$$

For $d > d_c$, we have a band of instable wavenumbers. The relation $\lambda = \lambda(k^2)$ is called the *dispersion relation*. The maximum singles out the fastest growing mode. This one dominates the solution

$$\vec{W}(\vec{r}, t) = \sum_k c_k \exp(\lambda(k^2)t)$$

for large t . Note however, that in this case also non-linear effects will become important and thus will determine the final pattern.

In summary, we have found four conditions (10.0.1) - (10.0.4) for the Turing instability to occur. We now analyze the Schnackenberg-model in one spatial dimension. We already noted that $a + b > 0$ and $b > 0$ for the steady state to make sense. From the phase plane we see that $f > 0$ for large u and $f < 0$ for small u . Hence, $f_u > 0$ around the steady state. Thus, $b > a$.



All in all, there are four relations:
 $f_u, f_v > 0$ and $g_u, g_v < 0$.

$$\Rightarrow \quad A \sim \begin{pmatrix} + & + \\ - & - \end{pmatrix}$$

From condition (10.0.1) and (10.0.3), we now calculate that $d > 1$ in this case (the activation B diffuses faster in this model). In general, the conditions (10.0.1)-(10.0.4) define a domain in (a, b, d) -space, the *Turing space*, in

which the instabilities occurs. The structure of the matrix A tells us how this will happen: as u or v increases, u increases and v decreases. So, the two species will grow *out of phase*. If there is a fluctuation to a larger A-concentration, it would grow due to the autocatalytic feature. Locally this would inhibit B and it decreases strongly. However, because B is diffusing fast, it now is depleted from the environment and there A is not activated anymore. Therefore A goes down in the environment, whereas B is high. This is the basic mechanism for stripe formation.

In the Gierer-Meinhardt model, the two species grow *in phase*. When the autocatalytic species A grows, so does B, because A is the activator in this model. Now B diffuses out and suppressed A in the environment. This is an alternative mechanism for stripe formation.

The domain size p has to be large enough for a wavenumber $k = \frac{n\pi}{p}$ to be within the range of the unstable wavenumbers ($\gamma \sim L^2$):

$$\gamma L(a, b, d) < \left(\frac{n\pi}{p}\right)^2 < \gamma M(a, b, d)$$

where L and M can be calculated exactly. Typically, the mode which grows has $n = 1$.



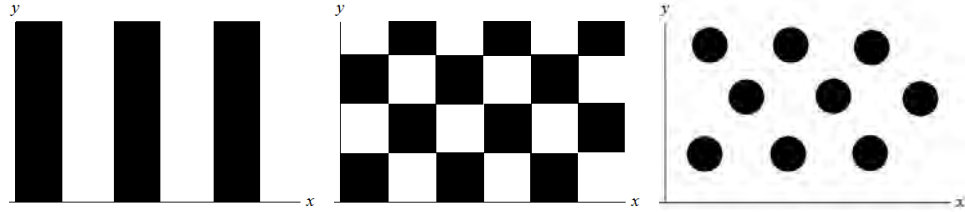
Whether the left or right solution occurs depends on the initial conditions. If the domain grows to double size, than γ changes by four ($\gamma \sim L^2$). p stays the same because it is measured in units of L . Now, the mode $n = 2$ behaves as shown in the following figures.



On this way, a growing system will develop a 1D stripe pattern.

In $D=2$ spatial dimensions, many more possible scenarios exist in a model-dependent manner: stripes (left), checkerboard (middle), hexagonal or tri-

angular (right) patterns, etc.



Today, the corresponding models are usually explored numerically, thus making it easy to also analyse the effects of the non-linear parts.